NASA Technical Memorandum 103968

An Exploratory Investigation of the Flight Dynamics Effects of Rotor RPM Variations and Rotor State Feedback in Hover

Robert T. N. Chen

September 1992

National Aeronautics and Space Administration

NASA Technical Memorandum 103968

An Exploratory Investigation of the Flight Dynamics Effects of Rotor RPM Variations and Rotor State Feedback in Hover

Robert T. N. Chen, Ames Research Center, Moffett Field, California

September 1992

National Aeronautics and
Space Administration

Ames Research Center
Moffett Field, California 94035-1000

LIST OF SYMBOLS

B_1	Engine damping, lb-ft-sec/rad
C_ζ	Lag damper coefficient, lb-ft-sec/rad
e_ζ	Lag hinge offset, ft
Hp	Shaft horse power
I_{bS}	$= I_\zeta + 2e_\zeta M_\zeta + m_\zeta e_\zeta^2$, blade moment of inertia about rotor shaft, slug-ft^2
I_H	Moment of inertia of the rotor hub, slug-ft^2
I'_R	$= I_H + N\, I_{bS}$
I_{eq}	Equivalent polar moment of inertia of engine/drive train system (referenced to rotor shaft speed), slug ft^2
I_ζ	Blade moment of inertia about lag hinge, slug-ft^2
K_s	Rotor shaft torsional stiffness, lb-ft/rad
k_ζ	Lag damper spring constant, lb-ft/rad
M_ζ	Mass moment of rotor blade about the lag hinge, slug-ft
m_ζ	Mass of one blade from lag hinge to blade tip, slug
N	Number of blades
Q_A	Total aerodynamic torque of all blades about the rotor shaft, lb-ft
$Q_{\zeta,A}$	Aerodynamic torque of one blade about the rotor shaft, lb-ft
Q_ζ	Total torque on a blade about the lag hinge (aerodynamics and lag damper contribution), lb-ft
Q_E	Engine torque (referenced to power turbine shaft speed), lb-ft
r	Aircraft yaw rate, rad/s
r_g	Engine to rotor nominal rpm ratio
v	Inflow velocity, ft/s

w	Aircraft body-axis vertical velocity, ft/s
ψ	Rotor hub angular displacement, rad
ψ_1	Gear box side of the rotor shaft angular displacement, rad
β	Flapping displacement (positive upward), rad
$\dot{\beta}$	Flapping rate, rad/s
ζ	Lead-lag displacement (positive against rotor rotation), rad
$\dot{\zeta}$	Lead-lag rate, rad/s
Ω	Rotor rotational speed, rad/s
θ_o	Collective pitch input, deg
δ_p	Pedals displacement, in.

SUMMARY

This paper presents the results of an analytical study conducted to investigate airframe/engine interface dynamics, and the influence of rotor speed variations on the flight dynamics of the helicopter in hover, and to explore the potential benefits of using rotor states as additional feedback signals in the flight control system. The analytical investigation required the development of a parametric high-order helicopter hover model, which included heave/yaw body motion, the rotor speed degree of freedom, rotor blade motion in flapping and lead-lag, inflow dynamics, a drive train model with a flexible rotor shaft, and an engine/rpm governor. First, the model was used to gain insight into the engine/drive train/rotor system dynamics and to obtain an improved simple formula for easy estimation of the dominant first torsional mode, which is important in the dynamic integration of the engine and airframe system. Then, a linearized version of the model was used to investigate the effects of rotor speed variations and rotor state feedback on helicopter flight dynamics. Results show that, by including rotor speed variations, the effective vertical damping decreases significantly from that calculated with a constant speed assumption, thereby providing a better correlation with flight test data. Higher closed-loop bandwidths appear to be more readily achievable with rotor state feedback. The results also indicate that both aircraft and rotor flapping responses to gust disturbance are significantly attenuated when rotor state feedback is used.

INTRODUCTION

Dynamic interface problems involving the engine/fuel control and the rotor/drive train/ airframe have been encountered in the ground or flight testing of helicopters for a long time (refs. 1–4). They are often manifested in severe torsional oscillations in the helicopter rotor drive shaft. In addition, problems occur in the fuel control system (refs. 5 and 6), in multi-engine load sharing, excessive vibrations, overtorque, and as undesirable rotor speed variations in certain flight conditions such as during autorotational recoveries (ref. 7). These problems not only compromise structural integrity but also generate adverse effects on handling qualities of the aircraft. Until recently, these dynamic interface problems have received little attention by the airframe/flight control system designers because they tend to ignore the rotor speed degree of freedom, thus decoupling, by assumption, the effects of the engine/fuel control system on the flight dynamics of the helicopter. Although the engine/fuel control specialists have paid considerable attention to these problems, they utilize a sophisticated engine dynamic model (refs. 8 and 9) in conjunction with a rather rudimentary model for the helicopter rotor/airframe dynamics for the prediction of the overall system performance (refs. 6 and 10). As a result, the prediction of the engine/airframe coupling is often inadequate and the problems of dynamic incompatibility can sometimes surface later in the ground or flight tests, requiring costly modifications to "fix" the problems.

These problems are further exacerbated by recent design requirements, especially for military helicopters, for greater agility and maneuverability. To meet these requirements, a highly responsive engine and a highly responsive rotor speed governor are needed.The required expansion in the bandwidth of the fuel control system can introduce severe couplings with the lightly damped torsional dynamic modes of the rotor and drive train systems, compromising the stability margin.

Compounding the problem is the trend towards using composite rotor blades with attendant lower rotor system inertia. With reduced kinetic energy stored in the system, the rotor becomes more susceptible to large variations in its rotational speed during rapid maneuvers. These rotor speed transients, especially when combined with concern about overtorquing, can severely increase pilot workload and lead to underutilization of the maneuver capability of the aircraft.

Several studies and flight investigations of advanced engine control systems have been conducted in the past few years (refs. 11–13). These control systems generally incorporate lead compensation through load anticipation logic to enhance the bandwidth of the engine control system. In these investigations comprehensive nonlinear simulation models were usually used, thereby providing a detailed simulation of the coupled engine/airframe dynamics and the attendant aircraft handling qualities. However, the effects of key design parameters on the system stability and performance were not well defined. Further, the benefits of using rotor states as additional feedback variables were largely left unexplored.

A recent parametric optimization study (ref. 14) has indicated that significant improvements in helicopter agility and maneuverability can be achieved by continuously varying ("C-V") the rotor speed in high performance maneuvers typically encountered in ground attack and air combat missions. The C-V rotor control laws were designed, using a point mass representation of the equations of motion for the helicopter. Rotor speed was varied continuously as a function of airspeed, commanded load factor, and other lead signals such as control displacements and rates. The rotor speed was permitted to vary in the range of 90 to 120% of the nominal values. With such large variations in rotor speed, the effects on flight dynamics and the associated flying-qualities implications need to be better understood, if the full potential of maneuverability and agility improvements can be realized.

The objectives of this analytical study are therefore: (1) to take a new look at the airframe/drivetrain/engine dynamic coupling problem using a simplified parametric high-order model, (2) to determine, with the simplified model, the extent to which variations in rotor rotational speed influence the flight dynamics of the helicopter, and (3) to conduct an exploratory assessment of the benefits of using rotor states as additional feedback signals in the control system. The study therefore began with the development of a parametric high-order helicopter hover model, which includes both body motion, rotor/blade degrees of freedom, air mass dynamics, and engine/rotor speed governor dynamics. A linearized version of the parametric model was then used to examine the flight/propulsion system integration and associated flight dynamic behavior and to identify potential benefits of rotor state feedback.

Simplied Parametric High-Order Hover Model

The simplified parametric hover model developed and used in this study is based on references 15–18. The model was developed expressly for the coupled vertical/yaw motion of the helicopter in hover; therefore, the other four body-degrees-of-freedom (ref. 17) were not included. The equation for the vertical motion of the aircraft is identical to that listed in references 15 and 17, but the yaw equation is simplified from reference 17 using a stability derivative representation for the aerodynamic terms. The engine and rotor speed governor equations, which are similar to those used in reference 17, include a simple first order dynamic representation for the engine and a typical

proportional-plus-integral rotor speed governor. The drive train dynamic representation includes a lumped equivalent inertia of the engine and transmission, engine damping effect, and a flexible rotor shaft. The rotor blade dynamics are represented by the coupled flap-lag rigid blade equations of motion for the lag-flap-pitch hinge sequence (ref. 18) with co-located flap and lag hinges similar to a UH-60 rotor system. A slight modification to reference 18 was made to account for the spring effect of either an elastomeric lag damper or the compressibility effect of the hydraulic fluid of a conventional lag damper. The rotor speed equation was derived by the Lagrange method, using energy equations already provided in reference 18. This equation, along with the lead-lag equation, forms a "double pendulum" like expression for the rotor hub and the rotor blades. In this study, primarily interest is focused on the collective flapping and lead-lag modes in hover; therefore, interblade dynamic couplings are neglected. The equation representing the inflow dynamics is identical to that shown in reference 15, which considers only the thrust component of the air mass dynamics. In summary, this parametric nonlinear model consists of:

(a) helicopter vertical and yaw motion;

(b) rotor rotational degree of freedom;

(c) rotor blade motions in flapping and lead-lag;

(d) inflow dynamics;

(e) drive train with flexible rotor shaft; and

(f) engine dynamics/rotor speed governor.

A detailed description of the parametric model is given in reference 19. A linearized state equation of the nonlinear model, as shown in Appendix I, will be used later to examine the effects of rotor speed variations on flight dynamics and to investigate the potential benefits of rotor state feedback. For now, however, we will first examine the dominant first torsional mode of the engine/drive train/rotor system using the nonlinear parametric model just described.

Estimation of the Natural Frequency of the First Torsional Mode

The coupled engine/drive train/helicopter rotor has a lightly damped torsional mode, the natural frequency of which is typically much less than the rotational frequency of the main rotor. This mode is commonly called the first torsional mode (refs. 1 and 2), which involves primarily the opposing motion of the engine and the main rotor blades . Because of its relatively low frequency, it can interact with the fuel control system and at, a high loop gain, can cause system instability or limit cycles, as have been well documented in the literature (refs. 5 and 6). A notch filter is usually used in the fuel control system (ref. 20) to attenuate this mode. Therefore, a rapid and accurate estimation of the frequency of this mode is needed in the preliminary design of the fuel control law.

Simple models are available in the literature (refs. 2 and 21) to provide a rapid estimation of the natural frequency of the first torsional mode. Many years ago, Sanders (ref. 2) proposed a simple

model consisting of two masses with two series springs as shown in figure 1. One of the two "masses" represents the equivalent inertia of the engine plus drive train, and the other represents the torsional inertia of the rotor blades; the two springs represent the torsional stiffness of the rotor shaft and the centrifugal spring of the rotor blades. Sanders shows a good correlation of the prediction of the model with the test data of reference 1. More recently, Ockier (ref. 21) proposed a simple model, which consists of two masses with only a centrifugal spring, assuming a torsionally very stiff rotor shaft. Clearly, this is merely a special case of the Sanders model.

The simplified parametric model described in this paper, will now be used to provide an estimate of the natural frequency of the first torsional mode. By focusing only on the engine, drive train, and the rotor system (and thus neglecting other rotor dynamics and aircraft motion), a model which consists of three masses and two springs,as shown in figure 2, is obtained. The governing equations are:

$$I_{eq}\ddot{\psi}_1 + K_S(\psi_1 - \psi) + B_l r_g^2 \dot{\psi}_1 = r_g Q_E \tag{1}$$

$$I_R'\ddot{\psi} - N\left\{2\dot{\psi}e_\zeta M_\zeta \zeta\dot{\zeta} + \left(I_\zeta + e_\zeta M_\zeta\right)\ddot{\zeta} - e_\zeta M_\zeta \zeta\dot{\zeta}^2\right\} = K_S(\psi_1 - \psi) - Q_A \tag{2}$$

$$\ddot{\zeta} - \left(1 + \frac{e_\zeta M_\zeta}{I_\zeta}\right)\ddot{\psi} + \frac{e_\zeta M_\zeta}{I_\zeta}\zeta\dot{\psi}^2 = \frac{Q_\zeta}{I_\zeta} \tag{3}$$

where

$$I_R' = I_H + NI_{bS}$$

$$I_{bS} = I_\zeta + 2e_\zeta M_\zeta + m_\zeta e_\zeta^2$$

$$Q_A = NQ_{\zeta,A}$$

$$Q_\zeta = Q_{\zeta,A} - C_\zeta\dot{\zeta} - k_\zeta\zeta$$

Equations (2) and (3) reflect the double-pendulum like representation, as mentioned earlier, for the hub-blades system with a spring which includes both centrifugal and lag damper spring effects. The latter comes from the spring effect of either elastomeric lag damper or the compressibility effect of the hydraulic fluid of the conventional lag damper.

Linearizing the equations (1)–(3) at the reference equilibrium condition, $\dot{\psi}_1 = \dot{\psi} = \Omega_o$, $\dot{\zeta}(o) = \dot{\zeta}_o = 0$, $\zeta(o) = \zeta_o$, and retaining only the spring terms result in a set of six state equations. This set of six equations consists of three dynamic modes: the rigid body mode, the first torsional mode, and the second torsional mode as shown in figure 3. The rigid-body mode, with zero eigenvalues, represents the mode in which the engine, rotor hub, and the blades rotate together as a rigid body, as can be seen by examining the associated eigenvector. The first torsional mode involves primarily the opposing motion of the engine and the rotor blades. More hub motion will participate in

this mode as the torsional stiffness of the rotor shaft increases or the equivalent inertia of the engine/drive train system decreases. The second torsional mode involves primarily the hub and blades motion. Again, more engine motion will participate in this third mode as the torsional stiffness of the rotor shaft increases or the equivalent inertia of the engine/drive train system decreases. It can be shown (ref. 19) that the natural frequencies of these two torsional modes can readily be calculated using the quartic characteristic equation:

$$\lambda^4 + d_1\lambda^2 + d_o = 0 \tag{4}$$

where

$$d_1 = \frac{K_s}{I_{eq}} + \frac{K_s}{\Delta I_R'} + \frac{1}{\Delta I_\zeta}\left(e_\zeta M_\zeta \Omega^2 + k_\zeta\right)$$

$$d_o = \frac{K_s}{\Delta I_R'}\left(e_\zeta M_\zeta \Omega^2 + k_\zeta\right)\left[\frac{1}{\Delta I_\zeta}\left(1 + \frac{\Delta I_R'}{I_{eq}}\right) - \frac{N}{\Delta I_R'}\left(1 + \frac{e_\zeta M_\zeta}{I_\zeta}\right)^2\right]$$

$$I_R' = I_H + N\left(I_\zeta + 2e_\zeta M_\zeta + m_\zeta e_\zeta^2\right)$$

$$\Delta = 1 - \frac{N I_\zeta}{I_R'}\left(1 + \frac{e_\zeta M_\zeta}{I_\zeta}\right)^2$$

Table 1 shows a comparison of three estimates of the first torsional natural frequency of a modern medium weight helicopter using references 2 and 21, and equation (4). Available test data for the aircraft indicate the natural frequency of this mode to be at 17.2 rad/s. The calculation was performed both with and without considering the spring effects of the elastometric lag damper used for this aircraft. It is seen that inclusion of the spring effect of the elastomeric lag damper is very significant. Because of the relatively lower torsional stiffness of the main rotor shaft for this aircraft, the estimate from Ockier's model (ref. 21) is considerably higher than the test value, as expected. The estimate from equation (4) appears to be somewhat better than that from Sanders model (ref. 2), due to additional consideration of the hub inertia and inertial coupling associated with the double pendulum formulation. Additional correlations were performed using equation (4) with test data of another modern helicopter and the old test data of reference 1. The calculated results for the first torsional mode were also found to be in good agreement with the test values. It should be noted however, that when the hub inertia is very small, care must be exercised to properly account for inertia contributions from various rotor components in equations (1)–(3) to avoid numerically induced instability.

Equation 4 provides a good insight into the key parameters influencing the lightly damped first torsional mode, which, as described earlier, needs to be considered in the design of the engine fuel control system. Three major parameters, i.e, torsional stiffness of the rotor shaft, equivalent engine inertia, and rotor speed, were examined. Figure 4 shows the effect of the torsional stiffness of the rotor shaft on the natural frequencies of the first and the second torsional modes of the engine/drive

train/rotor system of the example helicopter (see table 1). As expected, the first torsional frequency approaches the estimated value using Ockier's model, as the torsional stiffness of the rotor shaft increases. It is also shown that the percentage increase in the frequency for the 2nd mode is much more drastic than for the first mode. The effect of engine/drive train inertia is depicted in figure 5. Increasing the equivalent engine inertia (i.e., engine/drive train inertia referenced to the main rotor speed to account for the difference in the engine speed and the main rotor speed) results in decreased frequency of the first torsional mode, while the frequency of the second torsional mode remains essentially unchanged. A reduction in the amount of 22% in the first torsional frequency will result for a 100% increase in the equivalent engine/transmission inertia (e.g., due to a growth in transmission). The effect of the variations in rotor rotational speed on the natural frequencies of the two torsional modes is shown in figure 6. Due to the decreased centrifugal spring effects of the rotor blades when the rotor rotational speed is decreased, both the frequencies of the two torsional modes decrease, with less percentage reduction for the first mode than the second. While the variations in rotor speed affect only slightly the two torsional modes (since the reduced centrifugal spring is only part of the spring system consisting also of rotor shaft stiffness, and the lag damper spring effects), they affect significantly the aircraft response bandwidth and control effectiveness as will be discussed next.

Some Effects of Rotor Speed Variations on Flight Dynamics

It has been observed for some time now that the effective vertical damping of the rotorcraft in hover appears to be considerably smaller than the predicted value based on constant rotor rotational speed (refs. 15, 22–24). Flight test experience has also indicated that the helicopter responses, especially in the pitch and roll axes, become considerably more sluggish, when the main rotor speed droops. Conversely, the aircraft appears to be more responsive as the rotor speed increases. This study shows that variations in rotor speed affect significantly the aircraft response bandwidth and control effectiveness. For example, as the rotor speed decays, the effective vertical damping (and thus the vertical response bandwidth) is reduced significantly. When the rotor rpm is drooped from the nominal operating setting, both the roll damping and roll control effectiveness are substantially reduced, resulting in a significant reduction in roll response bandwidth and roll control sensitivity. By symmetry, the pitch axis also exhibits similar characteristics in hover.

Figure 7 shows a comparison of the rate-of-climb responses to a step collective input for the linear models with constant rotor speed, varying rotor speed with a rotor-speed governor, and varying rpm without a governor. These linear models were derived from the the linear model shown in the Appendix I. The associated system eigenvalues are shown in table 2. The rotor speed governor is one of proportional plus integral type designed for the example helicopter. Its rpm regulation characteristics are shown in figure 8. From figure 7 and table 2, it is clear that the effective vertical damping is significantly smaller (about 17%) for the varying rpm,with a governor, than for the constant rotor-speed case. A comparison of the vertical acceleration responses is shown in figure 9. Again, the response for the varying rpm case (with a governor) is considerably different than the constant rpm case, both in the initial transient and thereafter. The transient behavior has been shown previously (ref. 15) to be a result of the coupled inflow and flapping dynamics. The flattened response following the initial transient, which the varying rpm model predicts, is typically seen in flight test data (see fig. 10). The flattened acceleration response is a result of the rotor thrust which is shaped by the

slow-down-then-speed-up response characteristics of the rotor speed (fig. 8). Note that the predicted response can be expected to improve further when allowing for the feedforward effects from collective input to the fuel control unit, a feature that the test aircraft of figure 10 had. This is depicted in figure 11, in which the calculated normal acceleration responses to a step fuel flow are included. This flattened acceleration response to collective input, has not been predicted with a constant rotor-speed models (refs. 15 and 23). Although improvements in aerodynamic representation were considered in reference 23, the effects due to rotor speed variations were not addressed.

The effect of rpm variations on roll damping and roll control effectiveness was calculated using the simplified rotor equations of reference 16. Some results are shown in figures 12(a) and 12(b) respectively for the cases with and without collective retrimmed. In actuality, the situation probably resides somewhere between the two extreme cases. For both cases, the control effectiveness is approximately proportional to the square of the rpm ratio; however, for roll damping, the two cases are different as indicated in the figures. In figure 12(b), data from a comprehensive simulation model are also shown. This comprehensive helicopter nonlinear simulation model (ref. 25) includes a single main rotor model that considers rigid, hinge-restrained rotor blades with flap, lag, and torsional degrees of freedom. A three-state Pitt-Peters model for inflow dynamics is also included in this model. The quasi-steady values presented in figure 2(b) were reduced, using a low-frequency model reduction procedure commonly called residualization method, from high-order linear models generated from reference 25 at various rotor speed of interest (from 89% to 111% of the nominal rotor speed of 27 rad/s). These data from reference 25 correlate well with those generated from the simplified model of reference 16. The effect of rotor rpm droops on roll rate response to a step lateral stick input is shown in figures 13(a) and 13(b), which correspond to the two cases shown in figures 12(a) and 12(b). A first order approximation in the roll rate response was used in generating these plots. Note that for a first order approximation, the absolute value of the roll damping, Lp, is identical to the bandwidth of the roll rate response to lateral control input. It is seen therefore that the effects of rpm droops are twofold: (1) reduced bandwidth and (2) reduced control sensitivity. Both effects can contribute to the feel of sluggishness perceived by the pilot. Conversely, increased aircraft responsiveness may be perceived by the pilot when the rotor speed increases.

Rotor State Feedback

The idea of using rotor state feedback to achieve gust alleviation, helicopter attitude stabilization, and vibration reduction, has been around for a long time. In earlier days of helicopter development, mechanical devices and schemes, such as delta three (to change blade pitch with flapping displacement), pitch-cone coupling, and Oehmichen (changing blade pitch with flapping displacement of adjacent blade) are examples of using rotor state feedback for gust and vibration alleviation. In 1950, Miller (ref. 26) first analyzed the effects of feeding back the flapping displacement and flapping velocity to cyclic pitch on the stability and control characteristics of the helicopter. In this work, Miller also provided a comparative analysis of several mechanical stabilization devices involving use of rotor state feedback such as the Young stabilizer bar (ref. 27), the Kaman servo control, and the Hiller control rotor (ref. 28), then widely used by helicopter manufacturers. Later, rotor thrust and flap moment feedback concepts (refs. 29 and 30) were also proposed by researchers to lower gust response and to reduce dynamic rotor loads.

Following the introduction of the electronic flight control system for the helicopter in the late 1950s and early 1960s, rotor state feedback concepts were further pursued both analytically (refs. 31 and 32) and experimentally involving flight research (ref. 33). Hall and Bryson showed in their analytical work (ref. 31) that neglecting the rotor dynamics in the model used to design a high performance hover autopilot using linear-quadratic-Gaussian (LQG) methodology can result in unstable closed-loop response of the more completely modeled system that includes flapping dynamics. Use of rotor state feedback involving flapping displacement and flapping velocity eliminates the problem. Rotor state feedback is the essential part for the concept of Individual-Blade-Control advanced by Ham (ref. 32) for gust and vibration alleviation and attitude stabilization for helicopters. Flight investigation of rotor/airframe state feedback was conducted (ref. 33) to assess the feasibility of using rotor tip-path-plane motion to provide additional feedback signals to shape rotor and fuselage response. However, in these analytical and experimental studies, primary consideration has been focused on the flapping and flapping velocity as the only rotor state variables, in addition to the usual fuselage states, serving as feedback signals; use of other rotor state variables, such as blade lead-lag and rotor speed information, as additional feedback signals has largely been left unexplored. In this study, the effects of rotor state feedback are investigated using the high-order parametric model developed in this paper. Both flapping and lead-lag rotor states as well as other rotor states such as rotor speed and inflow will be considered as feedback signals to explore their potential benefits. Comparisons will be made in terms of closed-loop eigenvalues, frequency and transient responses for systems with and without rotor state feedback.

Effect of Rotor State Feedback on Stability

It is well known (refs. 31 and 34) that, without rotor state feedback (or high-order dynamic compensation), instability can develop when attempting to greatly enhance the bandwidth of the closed-loop system. The bandwidth of the closed-loop system can be enhanced by increasing the relative weighting of the state to control using the simple, full state feedback, linear-quadratic-regulator (LQR) control-law design method (ref. 31). In reference 31, the study used an analytical model that considers constant rotor speed and includes only flapping dynamics in the rotor subsystem. In what follows, the LQR method will be applied to the higher-order model developed in this paper,which includes variable rotor speed, flap and lead-lag dynamics, inflow, etc. In this exploratory study, perfect sensors (with no sensor dynamics or noise), ideal actuators (with no actuator dynamics, position or rate limits), and zero computational delay are considered. To evaluate the effects of achieving high bandwidth regulation without using rotor state feedback, two approaches are employed: (1) use a quasi-steady model, which assumes instantaneous rotor tilting, for LQR design and evaluate the resulting closed-loop system with the high-order model, and (2) use the high-order model in LQR design and evaluate the closed-loop system with rotor state feedback gains dropped.

Table 3 shows the full 10-state and the quasi-steady 5-state models and their respective system eigenvalues. The full 10-state model is that shown in the Appendix I, and the quasi-steady 5-state model is reduced from the full 10-state model, assuming instantaneous responses in blade flapping, lead-lag motion, and inflow variations. As can be seen from table 3, slight adjustments in the yaw/vertical modes and the engine/governor modes of the quasi-steady model are evident, reflecting the residualization effect for rotor and air-mass dynamics. The step responses of the rate-of-climb and the rpm to collective input are shown in figure 14 for the full and quasi-steady models. As

expected, these responses reflect that, as far as the low frequency region is concerned, the quasi-steady model matches well with the full-order model. However, with this quasi-steady model and with its attendant LQR gains(see table 4), the closed-loop system can become unstable when evaluation is made with the full-order model as shown in table 5. The instability occurs when the relative state to control weighting ρ increases, thereby increasing the bandwidth of the closed-loop system. From the associated eigenvector, it can readily be identified that the unstable mode is the collective flapping mode as shown in table 5 and figure 15. Table 5 lists the migration of all the eigenvalues, and figure 15 shows only the root locus of the flapping mode. The full-order model with its attendant full-state feedback gains increases the closed-loop bandwidth as the relative state to control weighting increases, as expected. This is also shown in table 5 and figure 15. However, these stable closed-loop system configurations become destabilized and eventually become unstable as the relative weighting increases, when the rotor state feedback gains are dropped. This is also shown in figure 15. Dropping off the rotor state feedback gains is the second approach, as mentioned earlier, of attempting to achieve a higher closed-loop bandwidth without using rotor state feedback. It is interesting to note that, although the two approaches of attempting to enhance closed-loop bandwidth without using rotor state feedback are distinctly different, the results are surprisingly similar.

It is important to assess the sensitivity of certain gains to the characteristics of the closed-loop system, since some of the feedback signals may not be readily accessible. It was found that dropping off the inflow gain and the integral-of-the rpm-error gain, individually and in combination, produce relatively insignificant changes in the closed-loop eigenvalues. Similarly, variations in lead-lag displacement and rate gains have very little influence on the closed-loop eigenvalues. However, it should be noted that this result is specifically for the use of collective lead-lag displacement and rate signals in the stability augmentation for vertical/yaw axes of interest in this paper. When augmentation in pitch and roll axes is the objective, cyclic lead-lag displacement and rate signals are essential rotor states to feedback in order to preserve system stability and achieve high bandwidth control-response and disturbance-rejection (ref. 35). In this study, it was found, as expected, that both the collective flapping-displacement gain and flapping-rate gain have a dramatic effect especially on the frequency and damping of the flapping mode as shown in figure 16. Availability of flapping rate signal is therefore essential for feedback to enhance the damping level of the flapping mode. State estimation methods, either model-based such as a Kalman filter or non-model-based such as a kinematic observer (ref. 36) may be required to provide this vital rate signal for feedback usage.

Effect of Rotor State Feedback on Transient Responses

The benefits of including rotor states as additional feedback signals, in addition to the usual fuselage states, can be seen clearly by examining the transient responses of the closed-loop system. Figure 17 shows the effect of rotor state feedback on vertical velocity transient response to a unit initial vertical velocity perturbation. As the relative state to control weighting increases (and thus the closed-loop bandwidth increases), the vertical velocity response becomes increasingly oscillatory when rotor state feedback is not used. Eventually, the closed-loop system becomes unstable as is clear from figure 15. With rotor state feedback, the vertical velocity response remains smooth while the response becomes faster and faster with increasing feedback gains. This quickened vertical velocity response is accomplished, of course, at the expense of the increased flapping response as shown in figure 18. However, with damping added to the closed-loop system by the flapping rate

feedback, it is seen that the peak flapping response is significantly smaller for the case with rotor state feedback than for the case without rotor state feedback. Also, as expected, the flapping response remains smooth as the system bandwidth increases.

The quickened vertical response has been achieved at the expense of the significantly increased responses in collective flapping motion. There are also significant increases in lead-lag motion and in the rotor speed variations as shown in figures 19 and 20. These responses are strongly influenced by the participation of the dominant collective flapping mode that is destabilized when rotor state feedback is not used. With rotor state feedback, both the lead-lag and rotor speed responses remain smooth as the level of augmentation is increased, in contrast to the oscillatory response in the case of no rotor state feedback. It is interesting to note, from figure 20, that, in contrast to the unaugmented case, the action of the augmented system is to allow an initial reduction in the rotor speed to provide the energy needed to achieve a quick gain in altitude. Thus, exchange of the kinetic energy of the rotor system for the potential energy of the aircraft has taken place. This exchange of energy is initiated by a rapid collective pulse type input via feedback control. This collective input, as shown in figure 21, provides a quick augmentation of thrust and causes the rotor speed to droop, before the engine begins to supply the power called for by the rotor speed governor.

At the high gain level of the augmented system without rotor state feedback, the collective input becomes very oscillatory due to the destabilized collective flapping mode as discussed earlier.

Effect of Rotor State Feedback on Disturbance Ejection

One of the major benefits of stability augmentation is the significant reduction in the aircraft and rotor responses to gust disturbances. Figure 22 shows the effect of rotor state feedback on gust response. This figure compares the vertical velocity responses to vertical gust input for open loop aircraft (the 10 state model) and the closed-loop systems with and without rotor state feedback. It shows that the attenuation in gust response with rotor state feedback increases both in magnitude and frequency range as the feedback gains increase. At a frequency of 1 rad/s for example, the attenuation amounts to slightly more than 10 db (3 times reduction) for the moderate gain level (fig. 22(b)), with more attenuation in the low frequency region than in the high frequency region. Although gust response attenuation is better in the low frequency region for the closed-loop system without using rotor state feedback (due partly to slightly higher gains as shown in table 4) compared with that having rotor state feedback, significant amplification takes place in the higher frequency region. Because of the destabilization trend with increased gains for the case without rotor state feedback (see fig. 15), the amplification in the higher frequency region, in the neighborhood of the flapping frequency, becomes greater as the gain level increases.

Figure 23 shows the effect of rotor state feedback on the flapping response to vertical gust input. The attenuation in the flapping response tends to shift to the higher frequency region as the gain level increases. Although there is a slight amplification in the very low frequency region (less than 0.2 rad/s), overall, considerable reduction in the flapping response to the vertical gust input is achieved when rotor state feedback is employed. Without rotor state feedback, the flapping response of the closed-loop system again exhibits a large amplification in the neighborhood of the flapping frequency, due to the destabilization of the flapping mode as the gain level increases.

The frequency responses of the lead-lag motion and rotor speed variations to vertical gust input are shown in figures 24 and 25. Although small in absolute terms (less than 0.1 deg lead-lag displacement per 10 ft/s vertical gust in amplitude), some amplification in lead-lag motion takes place for the augmented systems in the low frequency region. Part of the increased lead-lag motion is due to the increased rotor speed variations in that low frequency region, as can be seen in figure 25. As the feedback gains increase, the augmented system involving rotor state feedback achieves a slight attenuation in the higher frequency region. The augmented system without using rotor state feedback exhibits a substantial amplification in the high frequency region as the feedback gains increase due to the destabilized collective flapping mode.

CONCLUDING REMARKS

A parametric high-order hover model was developed for the investigation of flight dynamic effects of variations in rotor speed and rotor state feedback. The model included vertical/yaw motion of the aircraft, rotor speed degree of freedom, flap-lag dynamics, inflow dynamics, a drive train with flexible rotor shaft, and engine/governor dynamics. Using this model, an exploratory study was conducted which showed that

o With rotor speed variations considered, the aircraft vertical rate and vertical acceleration responses change significantly from those predicted with constant rotor speed. In particular, the effective vertical damping decreases significantly from that calculated with an assumption of constant rotor speed. The result thus appears to provide a better match with flight test data.

o Both pitch and roll control sensitivity and control response bandwidth decrease significantly with droops in rotor speed; conversely, control sensitivity and response bandwidth increases with increase in rotor speed. This result is in good agreement with effects observed in flight.

o The simple formula developed in this paper appears to provide an improved estimate of the natural frequency of the first torsional mode of the engine/drive train/rotor system; the simple formula also provides a good insight into the key parameters influencing this mode, which is important in dynamic integration of the engine and airframe system.

Using the LQR method, effects of rotor state feedback were investigated. The results showed that:

o With rotor state feedback, a higher closed-loop bandwidth appears to be more readily achievable than without using rotor state feedback; without rotor state feedback, instability occurs when attempting to increase the bandwidth of the closed-loop system.

o Another benefit of the rotor state feedback is the rejection of gust disturbances; both aircraft and some rotor responses to gust inputs are substantially attenuated when rotor state feedback is used. For the vertical gust examined in the paper, some gust response attenuation is achieved in flapping. However, amplifications, though small in absolute terms, can occur in such rotor states as lead-lag and rotor speed variations.

o For the vertical/yaw axes of the aircraft motion considered in this study, the results indicate that collective flapping and flapping rate are the two most effective rotor states for feedback; other rotor states, such as rotor speed, inflow, and lead-lag are much less effective. It is essential therefore that accurate measurements or estimates of the flapping and flapping rate signals be provided.

REFERENCES

1. Carpenter, P. J. and Peitzer, H. E.: Response of a helicopter rotor to oscillatory pitch and throttle movements. NACA TN 1888, June 1949.

2. Sanders, J. C.: Influence of rotor-engine torsional oscillation on control of gas-turbine engine geared to helicopter rotor. NACA TN 3027, Oct. 1953.

3. Keeling, J. C. and Kidd, D. L.: A study of turbine-powered helicopter drive system instability. 14th AHS Annual Forum, May 1958.

4. Anon, SAE ARP 704, Helicopter engine-rotor system compatibility. Society of Automotive Engineers, New York, June 1962.

5. Fredrickson, C.; Rumford, K.; and Stephenson, C.: Factors affecting fuel control stability of a turbine engine/helicopter rotor drive system. J. Am. Helciopter Soc., vol. 16, Jan. 1972, pp. 49-56.

6. Kuczynski, W. A.; Cooper, D. E.; Twomey, W. J.; and Howlett, J. J.: The influence of engine/fuel control design on helicopter dynamics and handling qualities. Proc. of the 35th AHS Annual Forum, May 1979.

7. Amer, K. B.; Prouty, R. W.; Korkosz, G.; and Fouse, D.: Lessons learned during the development of the AH-64A Apache attack helicopter. Proc. of the 48th AHS Annual Forum, June 1992.

8. Warwick, T. R.: Helicopter engine dynamics analysis. Paper No. 332, 25th AHS Annual Forum, May 1969.

9. Ballin, M. G.: A high fidelity real-time simulation of a small turboshaft engine. NASA TM-100991, July 1988.

10. Mihaloew, J. R. and Chen, R. T. N.: Rotorcraft flight-propulsion control integration. Vertiflite, vol. 30, no. 6, September-October 1984, pp. 45-47.

11. Howlett, J. J.; Morrison, T.; and Zagranski, R. D.: Adaptive fuel control for helicopter applications. J. AHS, vol. 29, no. 4, Oct. 1984, pp. 43-54.

12. Killion, S. W.: Flight tests of adaptive fuel control and decoupled rotor speed control systems. Proc. 45th AHS Annual Forum, May 1989.

13. Walsh, D. M.: Mission effectiveness testing of an adaptive electronic fuel control on an S-76A. Proc. 45th AHS Annual Forum, May 1989.

14. Schaefer, C. G., Jr. and Lutze, F. H., Jr.: Enhanced energy maneuverability for attack helicopters using continuous, variable (C-V) rotor speed control. Proc.1293-1303, AHS Annual Forum, May 1991.

15. Chen, R. T. N. and Hindson, W. S.: Influence of dynamic inflow on the helicopter vertical response. NASA TM-88327, June 1986.

16. Chen, R. T. N.: A simplified rotor system mathematical model for piloted flight dynamics simulation. NASA TM-78575, May 1979.

17. Talbot, P. D.; Tinling, B. E.; Decker, W. A.; and Chen, R. T. N.: A mathematical model of a single main rotor helicopter for piloted simulation. NASA TM-84281, Sept. 1982.

18. Chen, R. T. N.: Flap-lag equations of motion of rigid, articulated rotor blades with three hinge sequences. NASA TM-100023, Nov. 1987.

19. Chen, R. T. N.: A simplified parametric high-order hover model with applications. NASA TM in preparation.

20. Alwang, A. R. and Skarvan, C. A.: Engine control stabilizing compensation-testing & optimization. J. AHS, July 1977, pp. 13-18.

21. Ockier, C. J.: Engine rotor interaction: a dynamic analysis in hover. Master of Science Thesis, Department of Aerospace Engineering, University of Maryland, College Park, July 1990.

22. Feik, R. A. and Perrin, R. H.: Identification of an adequate model of collective response dynamics of a sea king helicopter in hover. Vertica, vol. 13, no. 3, 1989, pp. 251-265.

23. Houston, S. S. and Tarttelin, P. C.: Validation of mathematical simulations of helicopter vertical response characteristics in hover. J. AHS, vol. 36, no. 1, Jan. 1991, pp. 45-57.

24. Schroeder, J. A.; Watson, D. C.; Tischler, M. B.; and Eshow, M. M.: Identification and simulation evaluation of an AH-64 helicopter hover math model. AIAA-91-2877, presented at AIAA AFM Conf., August 12-14, 1991, New Orleans, LA.

25. Takahashi, M. D.: A flight-dynamic helicopter mathematical model with a single flap-lag-torsion main rotor. NASA TM-102267, Feb. 1990.

26. Miller, R. H.: A method for improving the inherent stability and control characteristics of helicopters. J. Aeronautical Sciences, June 1950, pp. 363-374.

27. Kelley, B.: Helicopter stability with Young's Lifting Rotor. S.A.E. Journal, December 1945.

28. Stuart, J.: The helicopter control rotor. Aeronautical Engineering Review, vol. 7, no. 8, August 1948, pp. 33-37.

29. Johnson, R. L. and Hohenemser, K. H.: On the dynamics of lifting rotors with thrust or tilting moment feedback controls. J. AHS, Jan. 1970, pp. 42-58.

30. Patthast, A. J. and Kerr, A. W.: Rotor moment control with flap-moment feedback. Preprint No. 842, Proc. AHS Annual Forum, May 1974.

31. Hall, W. E. and Bryson, A. E.: Inclusion of rotor dynamics in controller design. J. Aircraft, vol. 10, April 1973, pp. 200-206.

32. Ham, N. D.: Helicopter gust alleviation, attitude stabilization, and vibration alleviation using individual-blade-control through a conventional swash plate. 41st Annual AHS Forum, 1985.

33. Briczinski, S. J. and Cooper, D. E.: Flight investigation of rotor/vehicle state feedback. NASA CR-132546, 1975.

34. Chen, R. T. N. and Hindson, W. S.: Influence of high-order dynamics on helicopter flight-control system bandwidth. J. Guidance, Control, and Dynamics, vol. 9, no. 2, March-April 1986, pp. 190-197.

35. Takahashi, M. D.: Multivariable flight-control design using rotor-state feedback on an articulated rotor helicopter in hover and low speed flight. NASA TM in publication.

36. McKillip, R. M., Jr.: Kinematic observers for rotor control. Presented at the International Conf. on Rotorcraft Basic Research, Research Triangle Park, NC, Feb. 19-21, 1985.

APPENDIX I: LINEARIZED STATE EQUATION

The ten-state linear equation used in this study,

$$\dot{x} = Ax + Bu \qquad \text{(AI - 1)}$$

where the state x = col. ($\delta\Omega$, $\int \delta\Omega$, δw, r, δHP, $\dot{\zeta}$, $\dot{\beta}$, ζ, β, v), control u= col. ($\delta\theta_o$, δ_p),

A =

1.0D+03 *

Columns 1 thru 8							
-0.0110	0.0000	0.0000	0.0076	0.0001	-0.2024	0.0006	-1.0825
0.0010	0.0000	0.0000	0.0000	0.0000	0.0000	0.0000	0.0000
-0.0052	0.0000	0.0000	0.0025	0.0000	0.0024	-0.0002	0.0003
0.0000	0.0000	0.0000	-0.0003	0.0000	0.0000	0.0000	0.0000
-1.1071	-0.8304	0.0000	0.0000	-0.0033	0.0000	0.0000	0.0000
-0.0118	0.0000	0.0000	0.0089	0.0001	-0.2270	-0.0024	-1.2122
-0.0019	0.0000	0.0013	0.0033	0.0000	0.0032	-0.0239	0.0004
0.0000	0.0000	0.0000	0.0000	0.0000	0.0000	0.0000	0.0000
0.0000	0.0000	0.0000	0.0000	0.0000	0.0000	0.0010	0.0000
0.0144	0.0000	0.0070	0.0000	0.0000	0.0000	-0.1214	0.0000

Columns 9 thru 10	
0.0246	0.0000
0.0000	0.0000
-0.6018	0.0000
0.0000	0.0000
0.0000	0.0000
0.0264	0.0000
-0.8157	-0.0013
0.0000	0.0000
0.0000	0.0000
0.0000	-0.0104

B =

1.0D+03 *

-0.1477	0.0004
0.0000	0.0000
0.0402	0.0000
0.0000	0.0004
0.0000	0.0000
-0.1072	0.0000
0.6926	0.0000
0.0000	0.0000
0.0000	0.0000
1.8063	0.0000

was obtained by linearizing the parametric high-order hover model which was configured to simulate a utility helicopter similar to a UH-60 aircraft. For this aircraft, the rotor shaft was assumed to be torsionally rigid.

Table 1. Comparison of estimates of 1st torsional natural frequency of the example helicopter

Reference 21	Reference 2		Equation 4	
Without lag damper spring effect	With lag damper spring effect	Without lag damper spring effect	With lag damper spring effect	Without lag damper spring effect
23.23 rad/s	16.23	15.77	16.94	16.23

Parameter values

e_ζ = 2.875 ft
I_H = 120.89 slug-ft^2
I_{eq} = 1234.13 slug-ft^2
I_ζ = 803.52 slug-ft^2
M_ζ = 48.88 slug-ft
m_ζ = 7.59 slug
N = 4
K_s = 399,981.60 lb-ft/rad
k_ζ = 35981.00 lb-ft/rad
Ω = 30.25 rad/s

Table 2. Effects of lag damper characteristics and changing rpm on eigenvalues of the unaugmented example helicopter in hover

	Lag damper characteristics					
	ZETA, u.c. = 0.7*		ZETA, u.c. = 0.4		ZETA, u.c. = 0.1	
Modes	Const. rpm	Varying rpm	Const. rpm	Varying rpm	Const. rpm	Varying rpm
Vertical	–0.29	–0.24	–0.29	–0.24	–0.29	–0.24
Yaw/(rpm)	–0.34	–0.32/–0.58	–0.34	–0.32/–0.58	–0.34	–0.32/–0.58
Engine	–3.33	–3.33	–3.33	–3.33	–3.33	–3.33
Inflow	–14.38	–14.60	–14.42	–14.61	–14.44	–14.59
Collective flapping	–9.87 ± j 23.11	–9.71 ± j 23.01	–9.82 ± j 23.12	–9.71 ± j 23.01	–9.78 ± j 23.12	–9.65 ± j 22.95
Collective lead/lag	–4.99 ± j 5.17	–5.21/–232.27	–2.85 ± j 6.59	–9.51/–127.29	–0.72 ± j 7.14	–18.14 ± j 29.85

*Damping ratio of uncoupled lead-lag degree of freedom.

Table 3. Full 10-state and quasi-steady 5-state linear models and their eigenvalues

Full 10-state mode	Quasi-steady 5-state model (instantaneous rotor response)
$\dot{x} = Ax + B\underline{u}$	$\dot{x}_1 = A_Q x_1 + B_Q \underline{u}$
$x = \begin{bmatrix} x_1 \\ x_2 \end{bmatrix}, \; x_1 = \text{col.}(\delta\Omega \int\delta\Omega \; \delta w \; r \; \delta HP), \; x_2 = \text{col.}(\dot{\zeta} \; \dot{\beta} \; \zeta \; \beta \; v)$	$A_Q = A_{R_{11}} - A_{R_{12}} A_{R_{22}}^{-1} A_{R_{21}}$ $B_Q = B_{R_1} - A_{R_{12}} A_{R_{22}}^{-1} B_{R_2}$
$\underline{u} = \text{col.}(\zeta\theta_o \; \zeta p)$	
$A = \begin{bmatrix} A_{R_{11}} & A_{R_{12}} \\ A_{R_{21}} & A_{R_{22}} \end{bmatrix}, B = \begin{bmatrix} B_{R_1} \\ B_{R_2} \end{bmatrix}$	
Eigenvalues	
–0.29 ± j 0.01 (vertical/yaw)	–0.29/–0.31 (yaw/vertical)
–0.11 (rpm)	–0.11 (rpm)
–1.27 ± j 0.77 (engine/governor)	–1.39 ± j 0.71 (engine/governor)
–14.61 (inflow)	
–9.71 ± j 23.02 (flapping)	
–5.76/–231.97 (lag)	

Table 4. Feedback gain matrix, K_f

$$u = \begin{Bmatrix} \delta\theta o \\ \delta_p \end{Bmatrix} = -\kappa_f x$$

ρ	Feedback gains	ΔΩ	∫ΔΩ	δw	r	δHP	$\dot{\zeta}$	$\dot{\beta}$	ζ	β	ν
	For 5-state model	–0.0042	–0.0061	–0.0144	0.0002	0	0	0	0	0	0
		0.0002	0.0001	0	0	0	0	0	0	0	0
0.001											
	For 10-state model	–0.0023	–0.0059	–0.0139	–0.0006	0	0.0017	0.0119	0.0094	0.2261	–0.0009
		0.0002	0.0001	0	0.0008	0	–0.0001	0	–0.0003	–0.0003	0
	For 5-state model	–0.0161	–0.0132	–0.0334	0.0004	0	0	0	0	0	0
		0.0009	0.0004	–0.0001	0.0042	0	0	0	0	0	0
0.005											
	For 10-state model	–0.0098	–0.0128	–0.0327	–0.0022	0	0.0069	0.0272	0.0393	0.7139	–0.0014
		0.0008	0.0004	–0.0001	0.0042	0	–0.0007	–0.0001	–0.0016	–0.0013	0
	For 5-state model	–0.0252	–0.0185	–0.0476	0.0005	0	0	0	0	0	0
		0.0017	0	–0.0002	0.0083	0	0	0	0	0	0
0.01											
	For 10-state model	–0.0156	–0.0181	–0.0468	–0.0036	0	0.0101	0.0370	0.0613	1.1046	–0.0016
		0.0016	0.0007	–0.0002	0.0083	0	–0.0014	0.0002	0.0032	–0.0025	0

Table 5. Effect of rotor state feedback on closed-loop eigenvalues

LQR Method: $J = \int_0^\infty (x' \rho R_{xx} x + u' R_{uu} u) dt$

$R_{xx} = \mathrm{diag}([1.42, 0, 0.25, 142, 0, 0, 0, 0, 0, 0]), R_{uu} = I_2$

		$\rho = 0.001$		$\rho = 0.005$		$\rho = 0.010$	
Feedback gain design	Unaugmented eigenvalues	Evaluated with 5-state model	Evaluated with 10-state model	Evaluated with 5-state model	Evaluated with 10-state model	Evaluated with 5-state model	Evaluated with 10-state model
Design for 5-state model	–0.29 –0.31 –1.11 –1.40 ± j 0.71	–0.29 –0.68 ± j 0.77 –2.41 –4.98	–0.29 –0.66 ± j 0.77 –2.47 –3.08 –21.06 –4.83 ± j 23.84 –5.76 –232.37	–0.29 –0.68 ± j 0.79 –2.29 –11.38	–0.29 –0.66 ± j 0.78 –2.21 –4.89 –27.80 –0.62 ± j 26.23 –5.77 –233.50	–0.29 –0.68 ± j 0.79 –2.28 –16.12	–0.29 –0.66 ± j 0.78 –2.19 –5.38 –31.46 1.49 ± j 27.91 –5.78 –234.36
		With rotor state feedback	Without rotor state feedback	With rotor state feedback	Without rotor state feedback	With rotor state feedback	Without rotor state feedback
Design for 10-state model	–0.29 ± j 0.01 –1.11 –1.27 ± j 0.77 –14.61 –9.71 ± j 23.02 –5.76 –231.97	–0.29 –0.65 ± j 0.77 –2.33 –3.73 –16.16 –10.33 ± j 23.87 –5.77 –232.02	–0.29 –0.67 ± j 0.78 –2.35 –3.07 –20.79 –4.98 ± j 23.82 –5.76 –232.20	–0.29 –0.65 ± j 0.78 –2.18 –5.65 –20.20 –11.99 ± j 26.02 –5.87 –232.24	–0.29 –0.67 ± j 0.80 –2.11 –4.83 –27.31 –0.78 ± j 26.21 –5.77 –232.91	–0.29 –0.65 ± j 0.78 –2.17 –6.25 –23.17 –13.32 ± j 27.58 –5.74 –232.50	–0.29 –0.67 ± j 0.81 –2.09 –5.33 –30.87 1.38 ± j 27.91 –5.78 –233.47

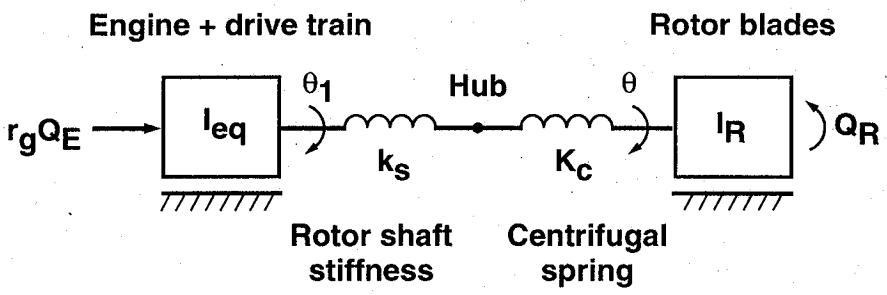

Figure 1. Sanders model.

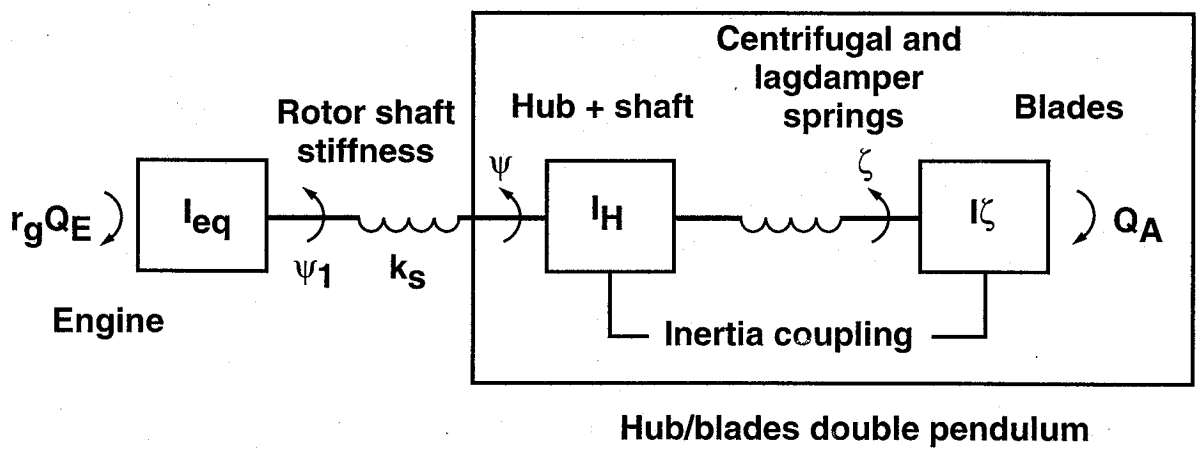

Figure 2. A simple model consisting of a mass, a flexible rotor shaft, and a double pendulum for hub/blades.

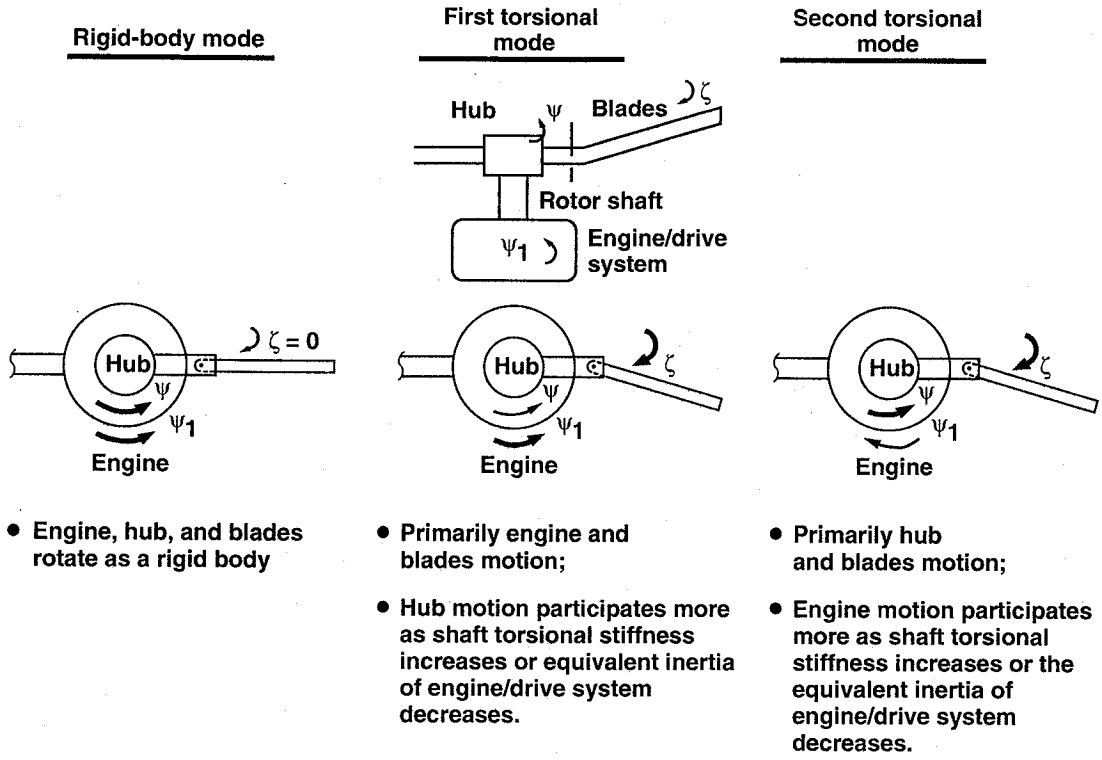

Figure 3. Torsional modes of the simplified engine/drive train/rotor model.

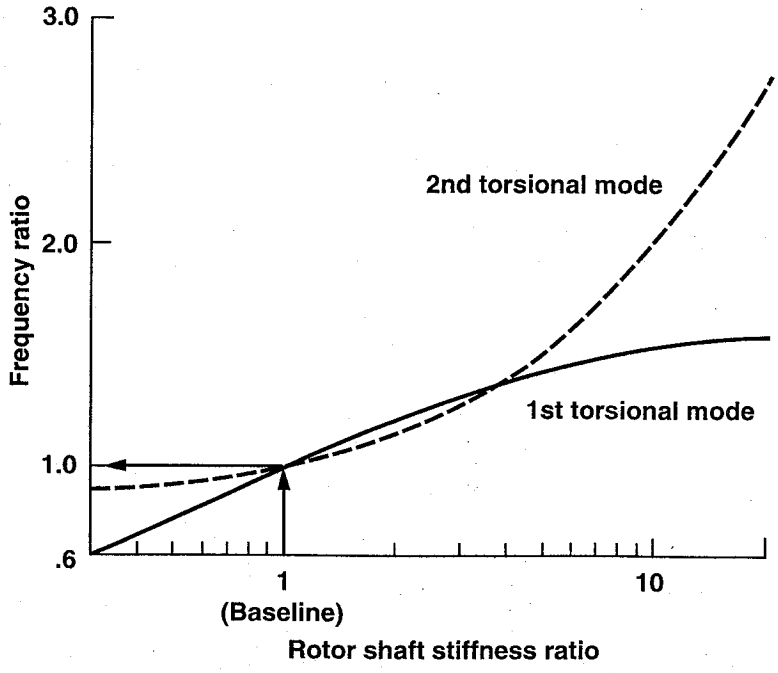

Figure 4. Effect of rotor shaft stiffness on engine/drive train/rotor torsional modes.

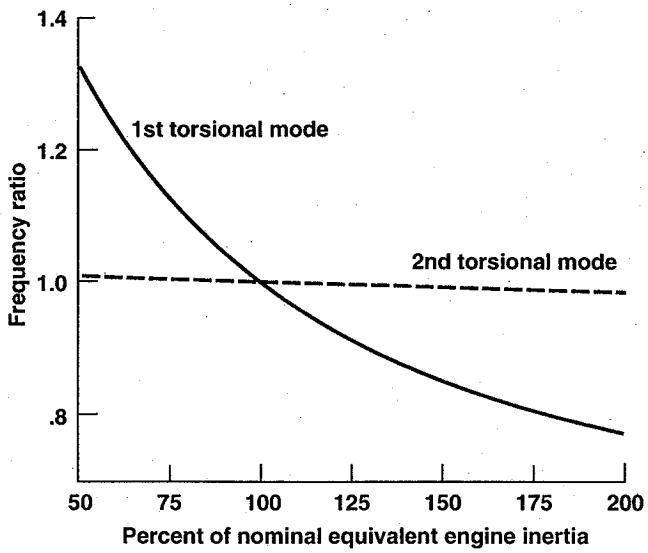

Figure 5. Effect of engine/drive train inertia on engine/drive train/rotor torsional modes.

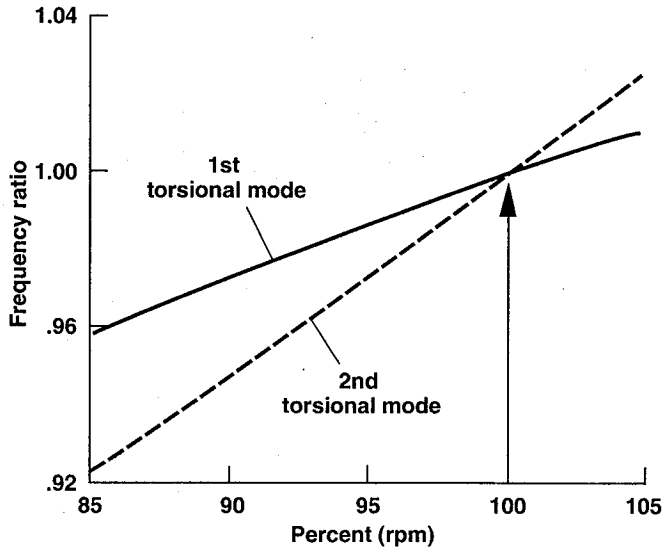

Figure 6. Effect of rotor rpm variations on torsional modes.

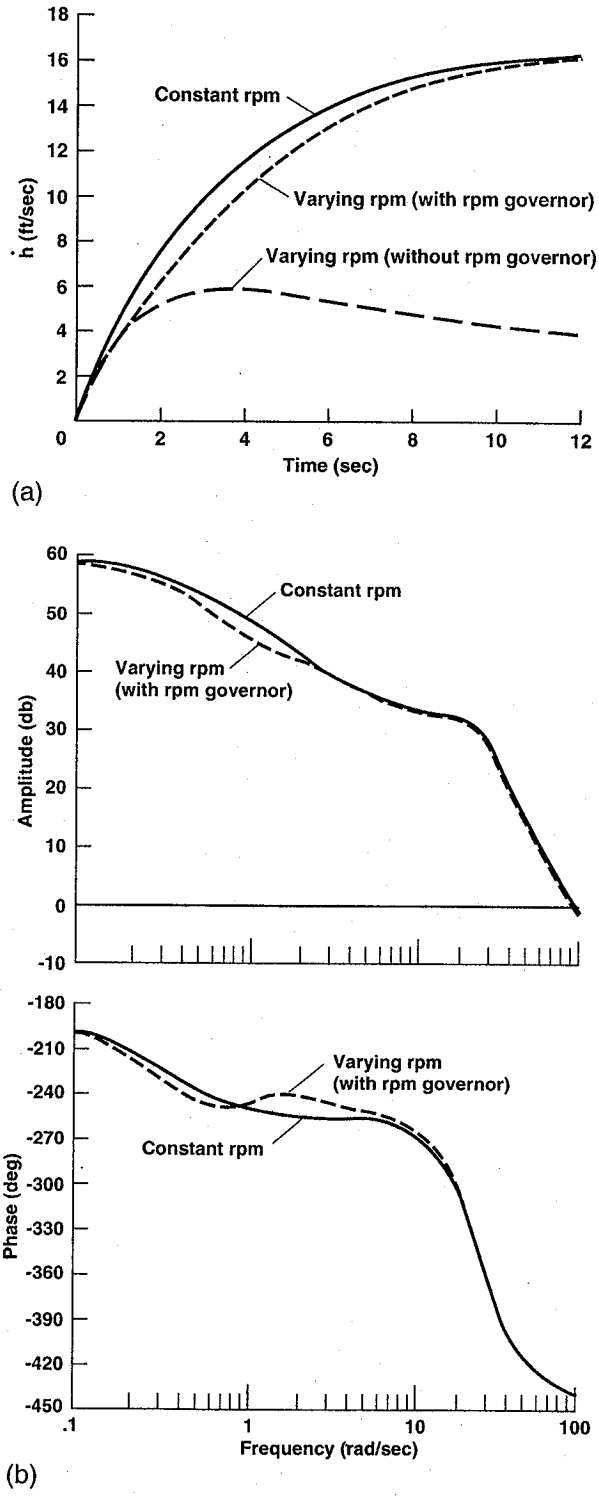

Figure 7. Comparison of rate-of-climb responses to collective input: a) transient responses to a step (1 deg) input, b) frequency responses.

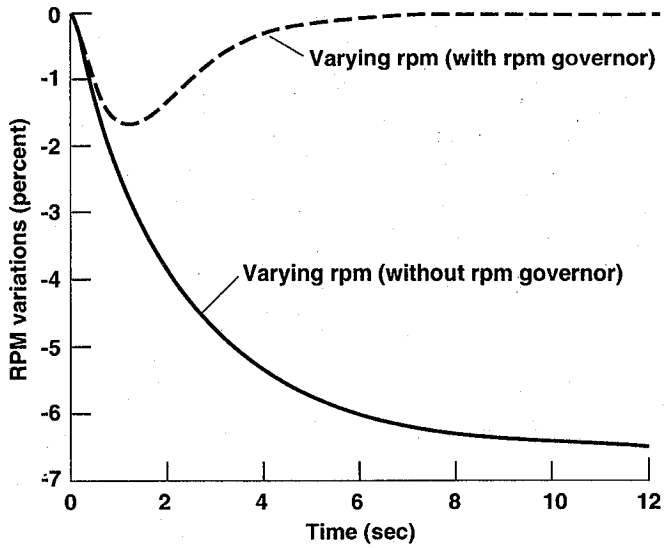

Figure 8. Comparison of rpm responses to step (1 deg) collective input.

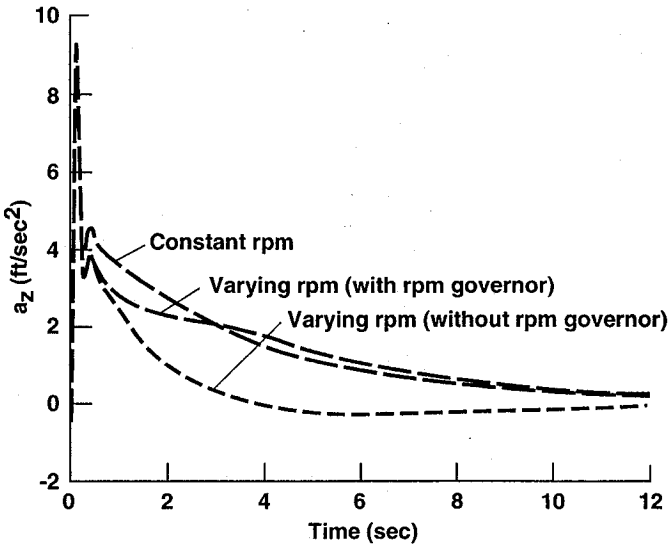

Figure 9. Comparison of vertical acceleration responses to step (1 deg) collective input.

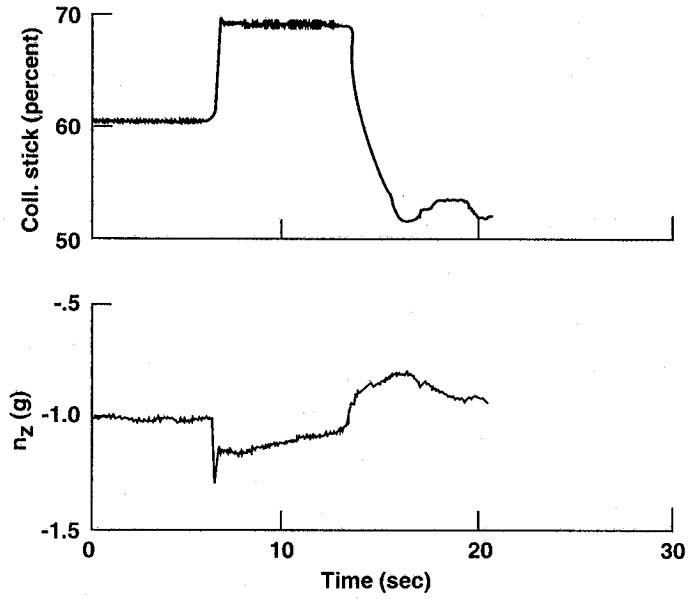

Figure 10. Typical flight test data showing acceleration response to a step like collective input in hover (UH-60 test data).

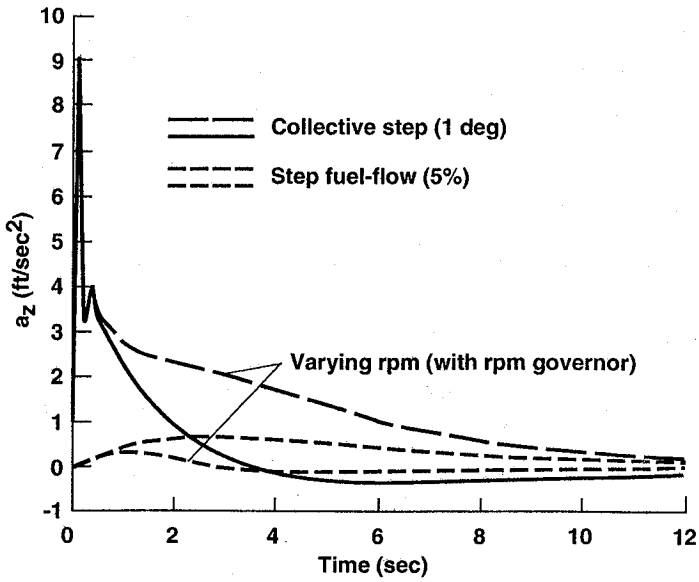

Figure 11. Comparison of vertical acceleration responses to step (1 deg) collective and fuel-flow inputs.

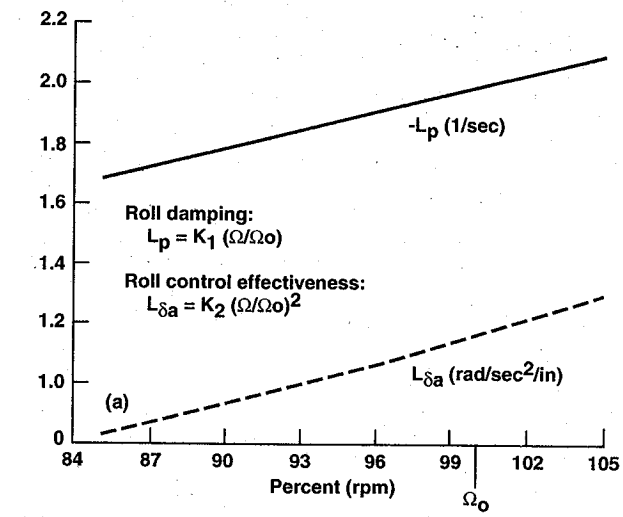

(a)

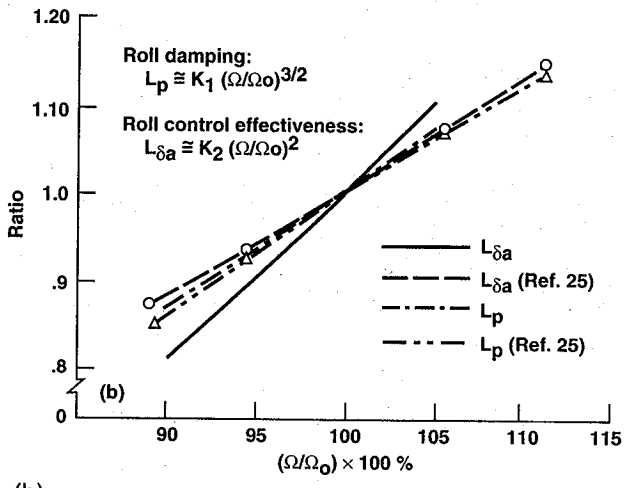

(b)

Figure 12a). Effect of rpm variations on roll damping and roll control effectiveness in hover (without collective retrimmed), b) effect of rpm variations on roll damping and roll control effectiveness in hover (with collective retrimmed).

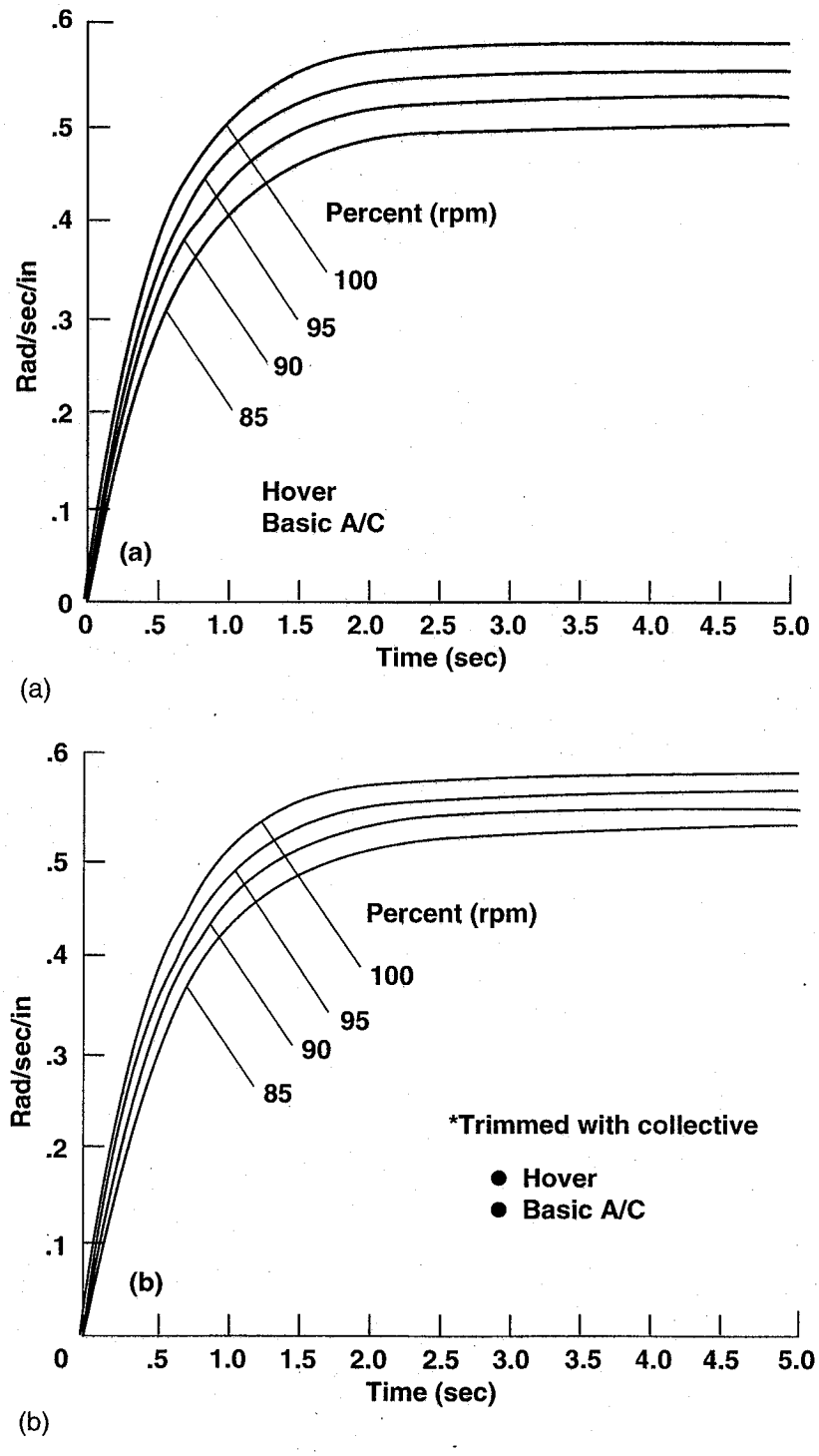

Figure 13. Effect of rpm droop on roll rate response in hover: a) without collective retrimmed, b) with collective retrimmed.

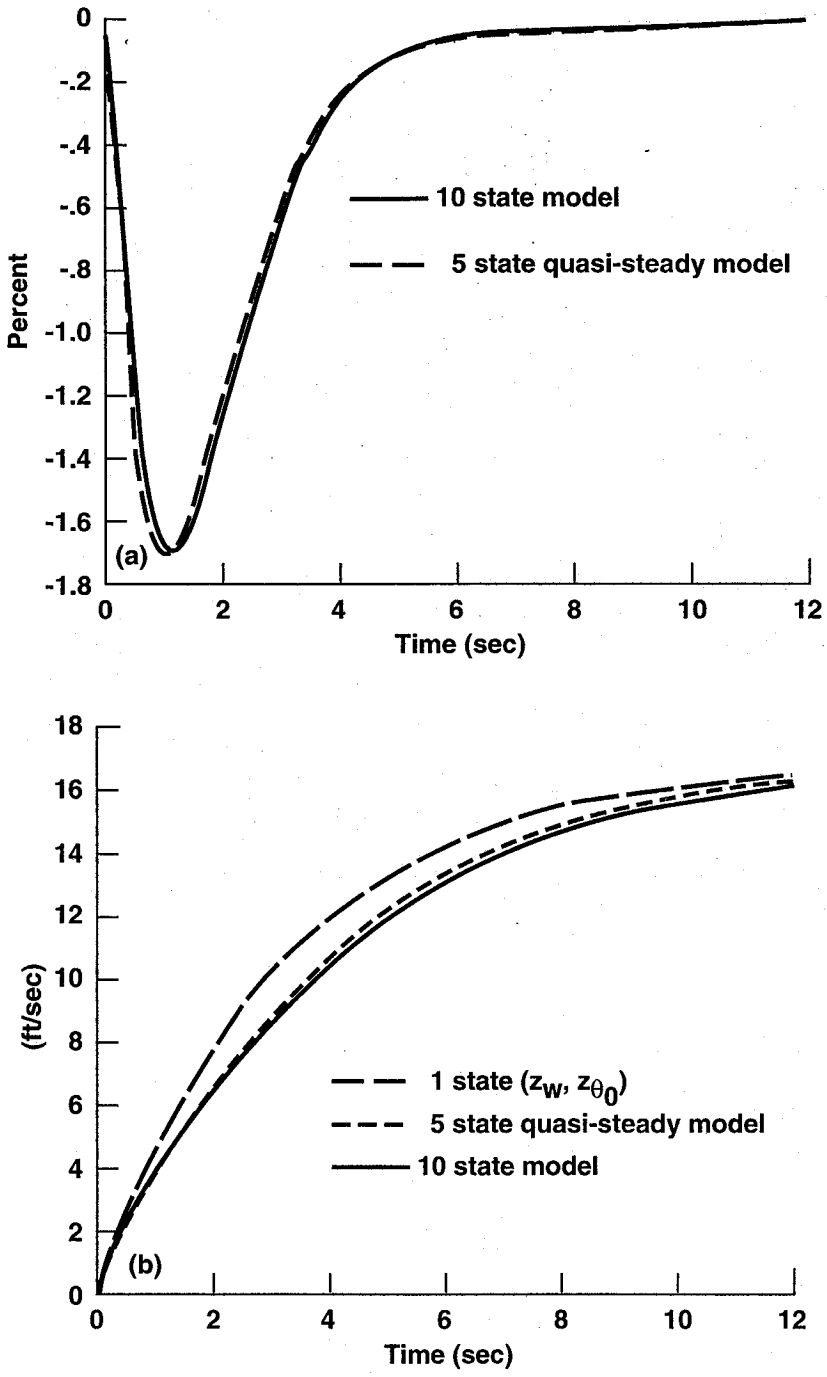

Figure 14a). Comparison of rpm responses to step (1 deg) collective input, b) comparison of rate-of-climb responses to step (1 deg) collective input.

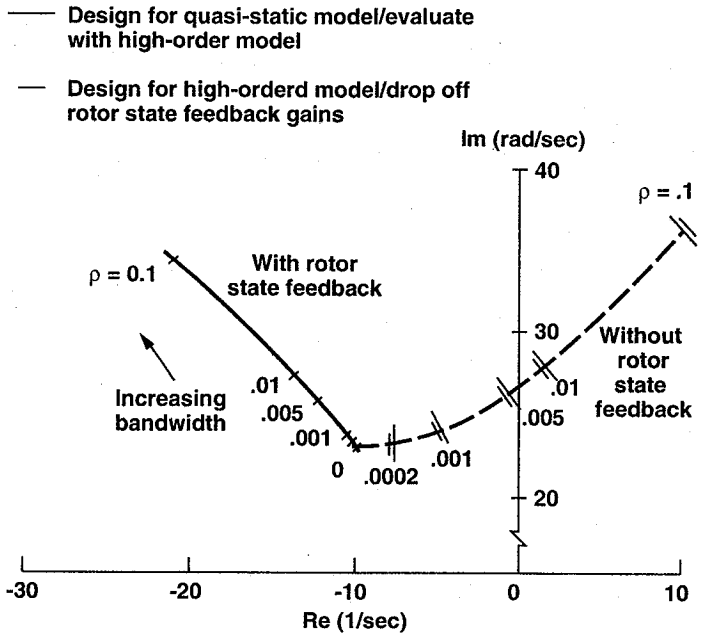

Figure 15. Eigenvalues of the flapping mode with and without rotor state feedback.

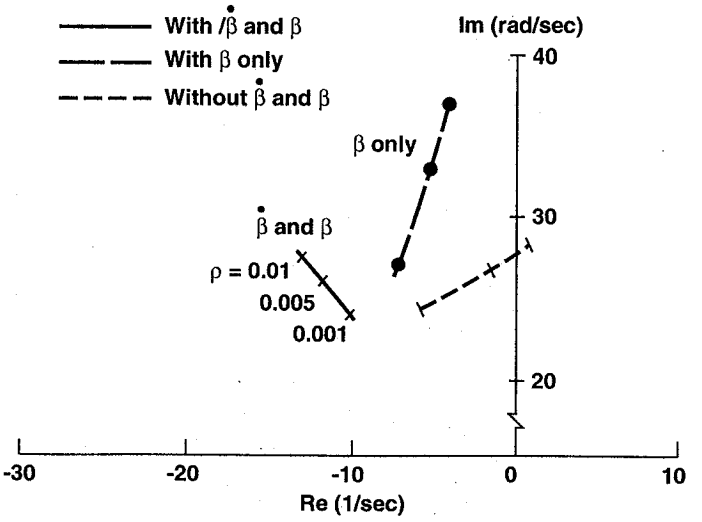

Figure 16. Effect of flapping and flapping velocity feedback on the flapping eigenvalues.

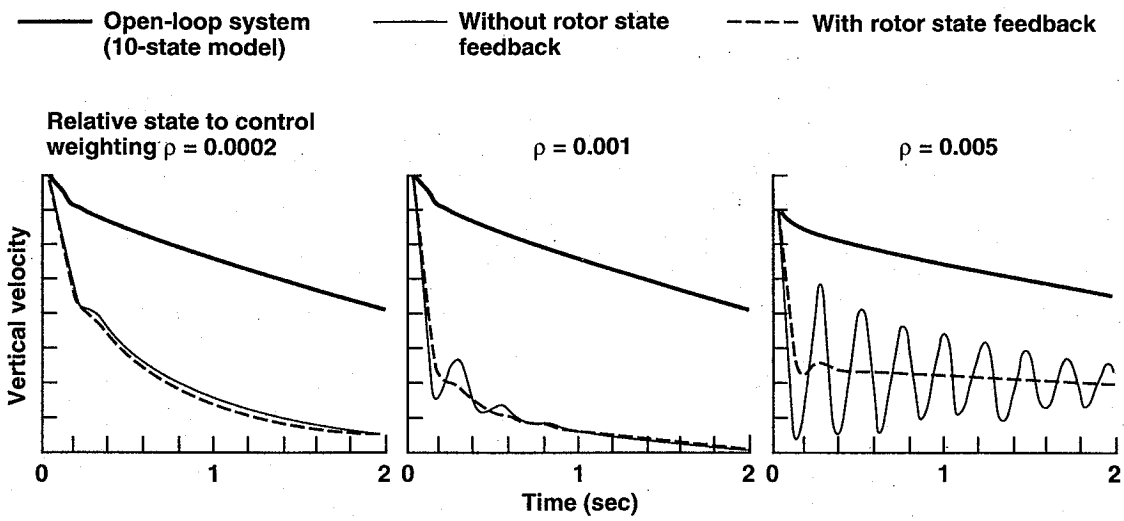

Figure 17. Effect of rotor state feedback on vertical velocity transient response.

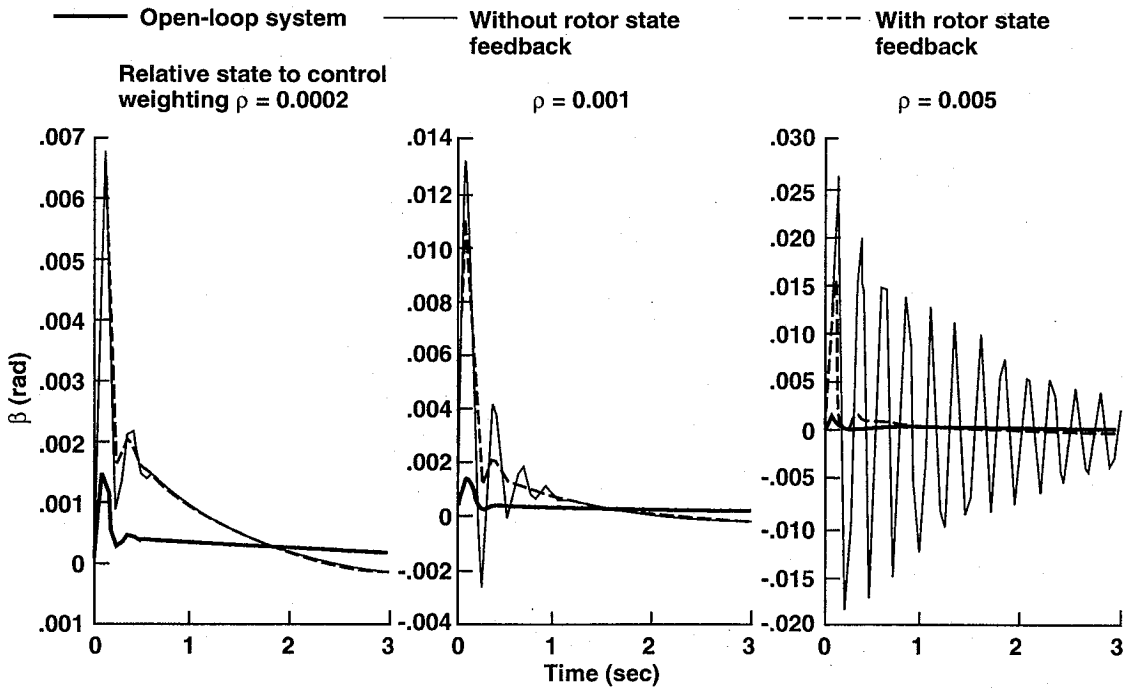

Figure 18. Effect of rotor state feedback on transient response of flapping.

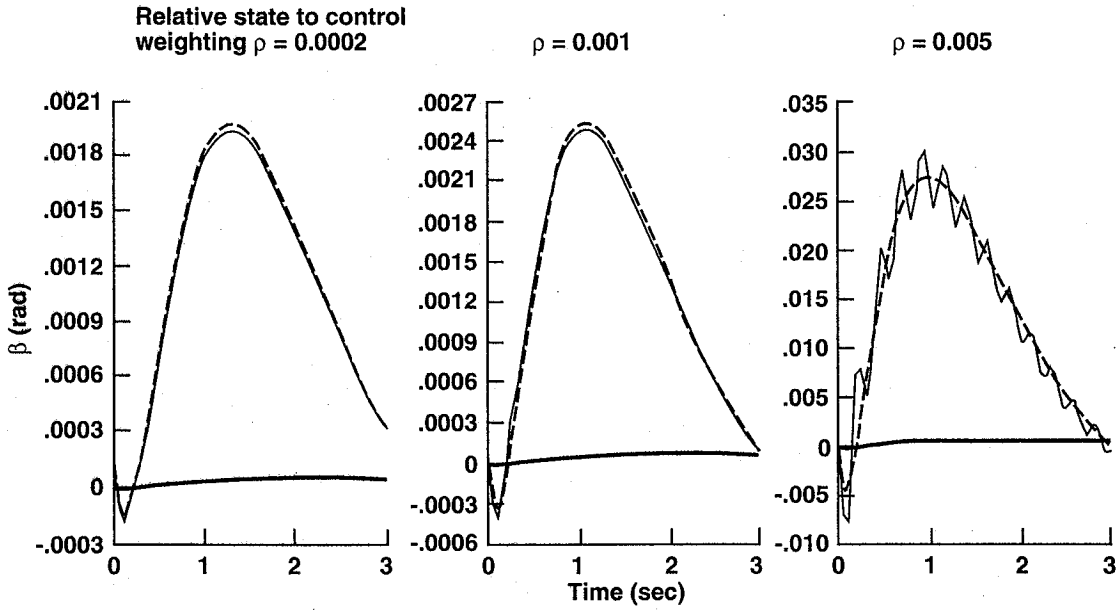

Figure 19. Effect of rotor state feedback on collective lead-lag transient response.

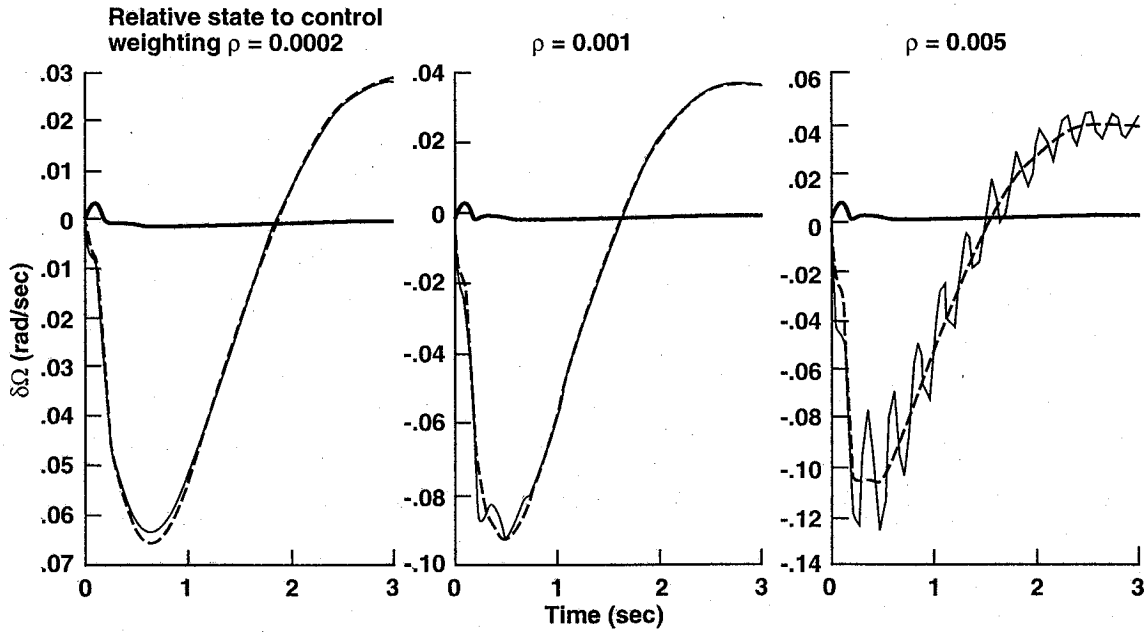

Figure 20. Effect of rotor state feedback on transient response of rotor speed variations.

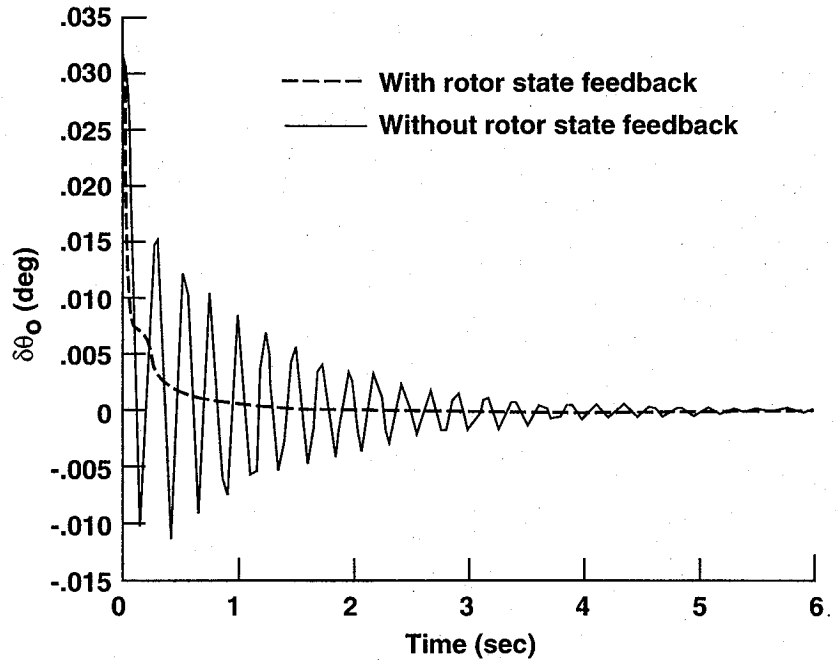

Figure 21 Effect of rotor state feedback on collective input due to feedback control ($\rho = 0.005$).

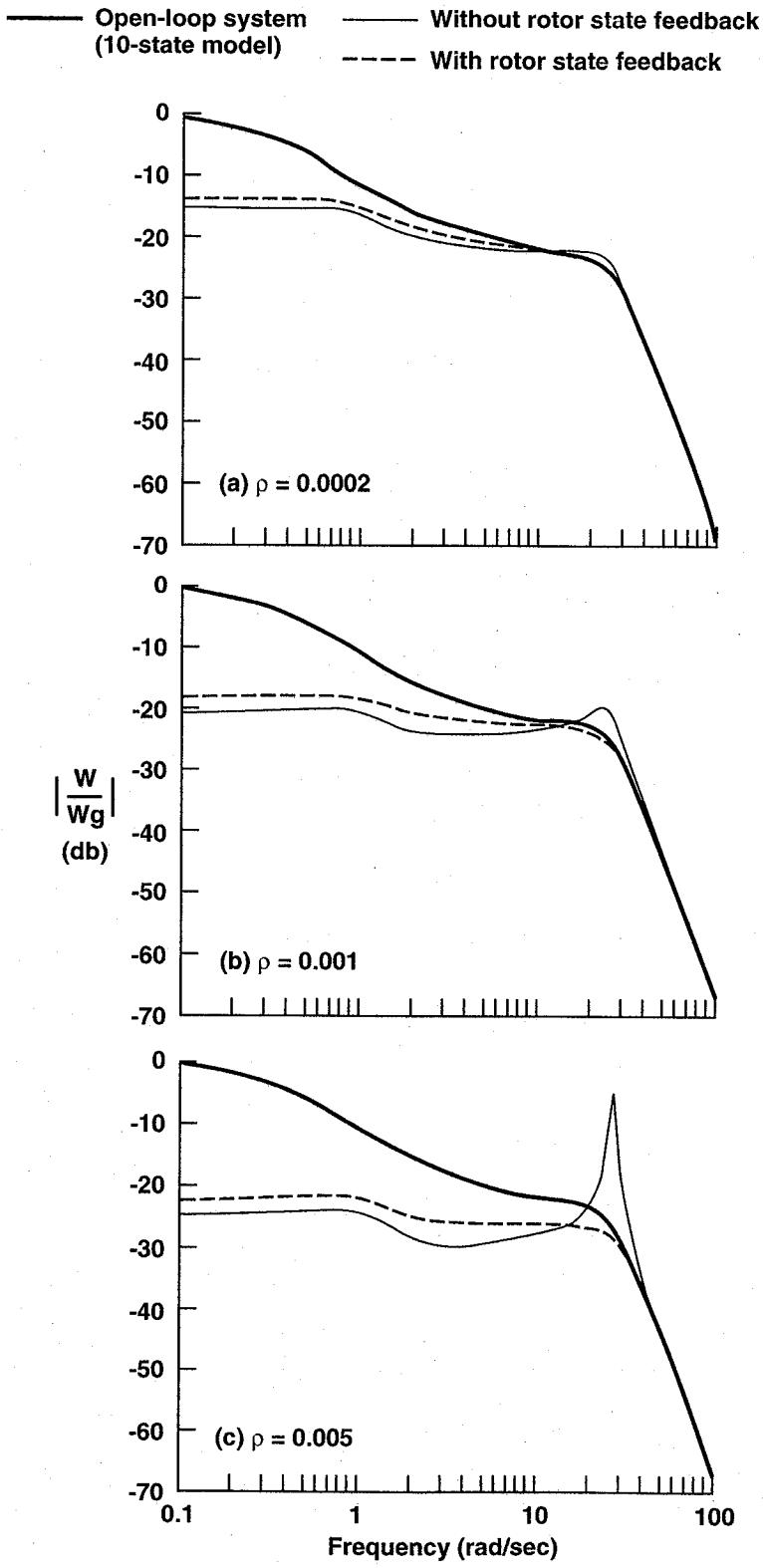

Figure 22. Effect of rotor state feedback on gust response: frequency response of vertical velocity to vertical gust input.

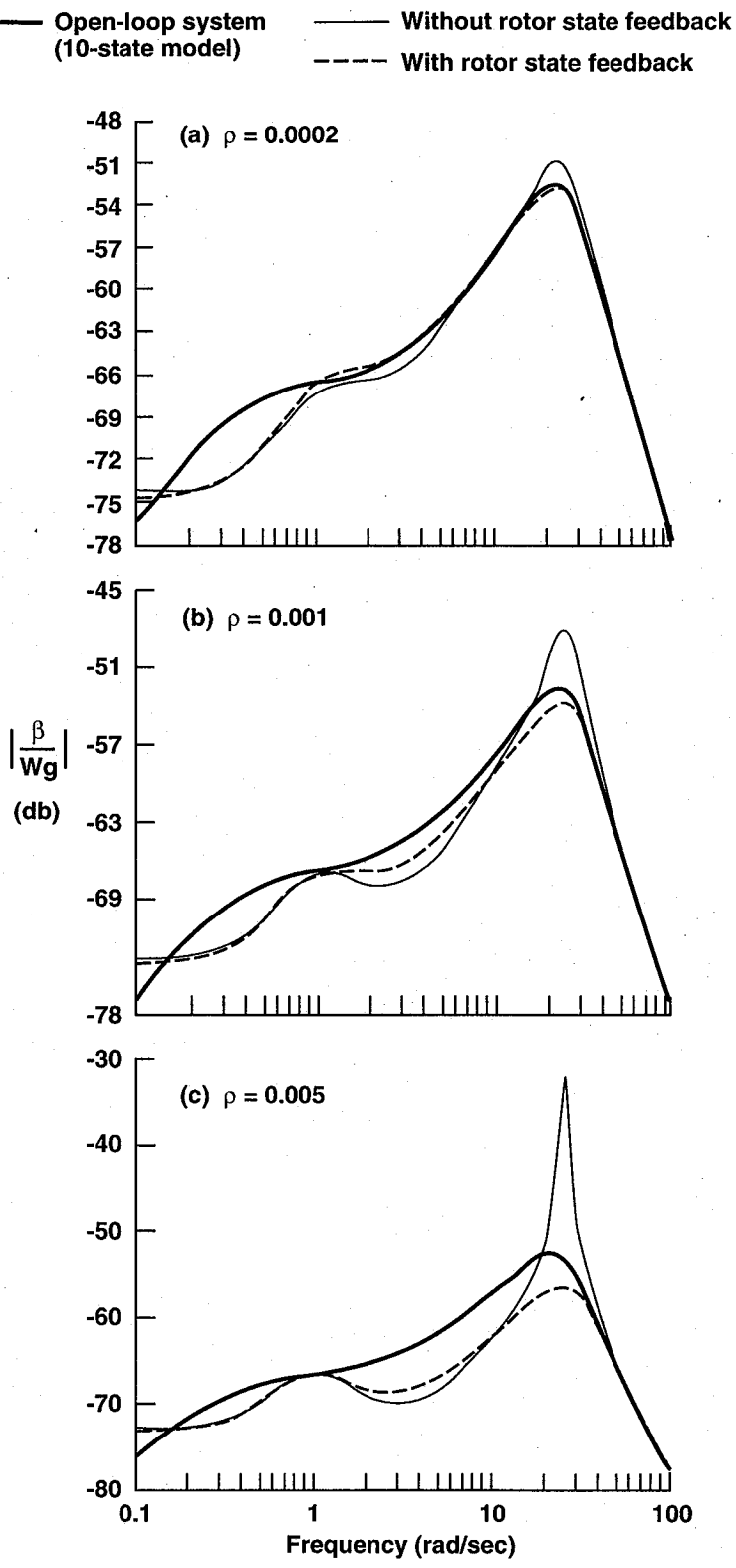

Figure 23. Effect of rotor state feedback on gust response: frequency response of flapping to vertical gust input.

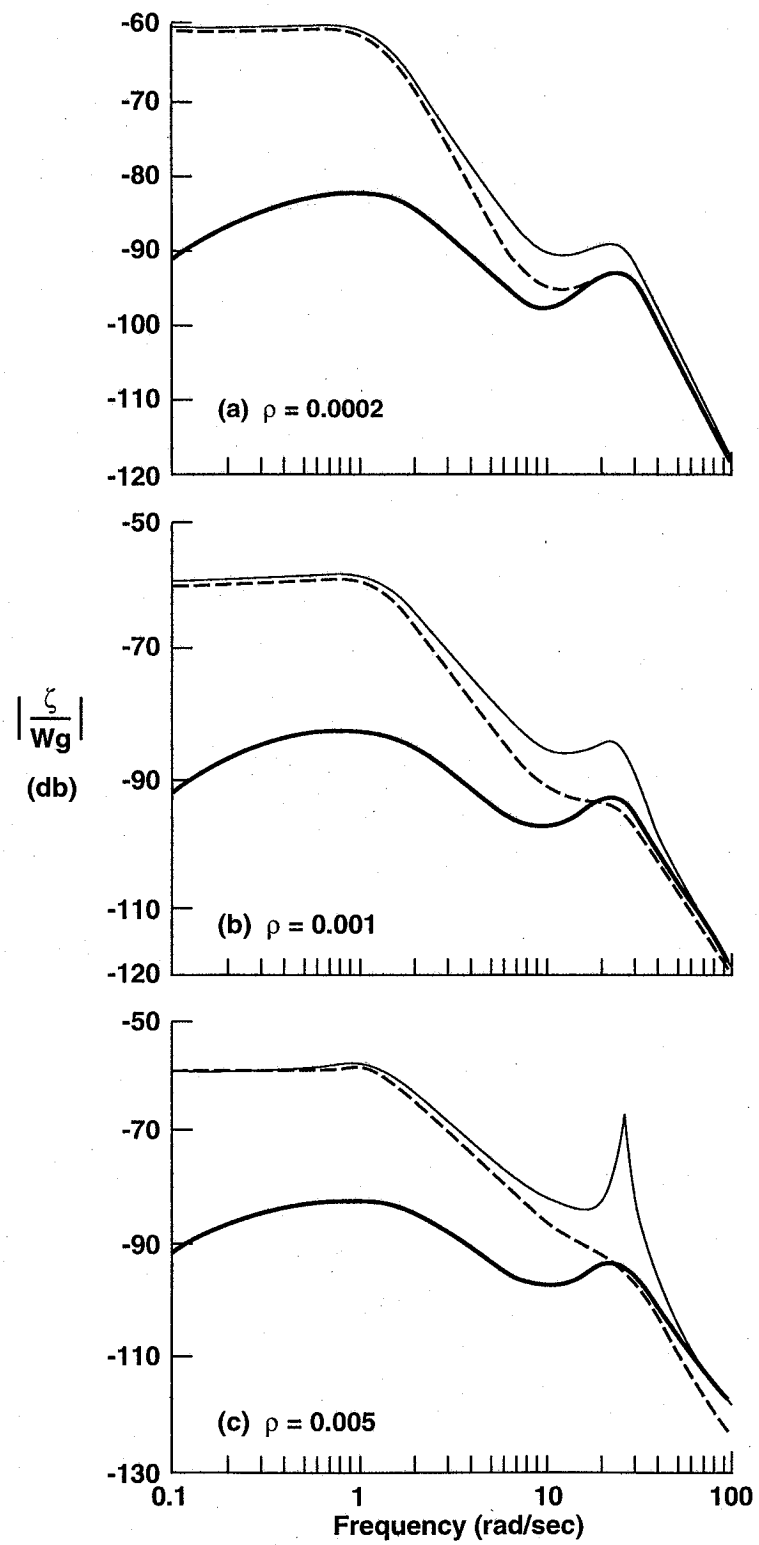

Figure 24. Effect of rotor state feedback on gust response: frequency response of lead-lag to vertical gust input.

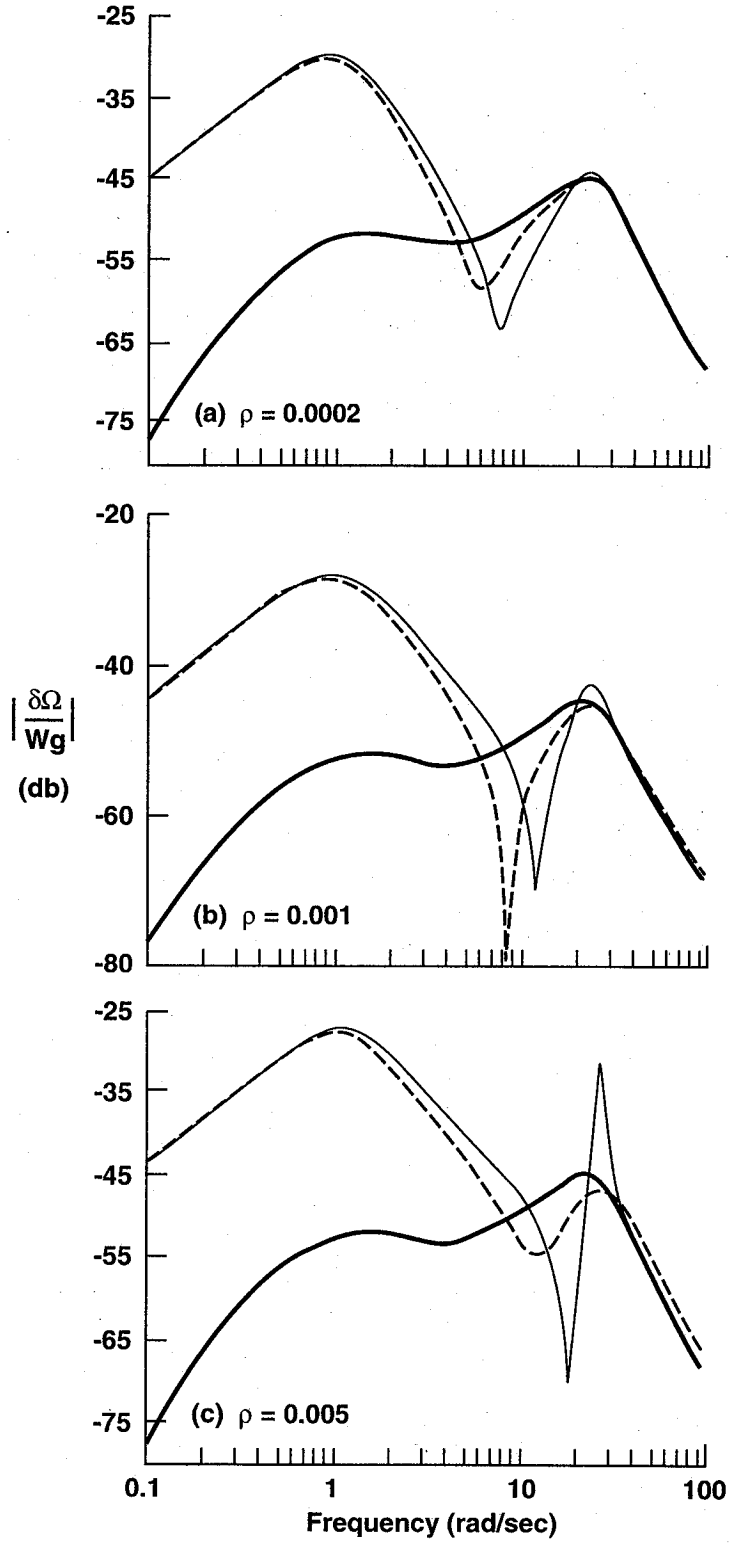

Figure 25. Effect of rotor state feedback on gust response: frequency response of rotor speed variations to vertical gust input.

REPORT DOCUMENTATION PAGE

Form Approved
OMB No. 0704-0188

1. AGENCY USE ONLY *(Leave blank)*	2. REPORT DATE	3. REPORT TYPE AND DATES COVERED
	September 1992	Technical Memorandum

4. TITLE AND SUBTITLE

An Exploratory Investigation of the Flight Dynamics Effects of Rotor RPM Variations and Rotor State Feedback in Hover

5. FUNDING NUMBERS

505-59-36

6. AUTHOR(S)

Robert T. N. Chen

7. PERFORMING ORGANIZATION NAME(S) AND ADDRESS(ES)

Ames Research Center
Moffett Field, CA 94035-1000

8. PERFORMING ORGANIZATION REPORT NUMBER

A-92173

9. SPONSORING/MONITORING AGENCY NAME(S) AND ADDRESS(ES)

National Aeronautics and Space Administration
Washington, DC 20546-0001

10. SPONSORING/MONITORING AGENCY REPORT NUMBER

NASA TM-103968

11. SUPPLEMENTARY NOTES

Point of Contact: Robert T. N. Chen, Ames Research Center, MS 211-2, Moffett Field, CA 94035-1000
(415) 604-5008
Paper given at 18th European Rotorcraft Forum, Avignon, France, Sept. 15-18, 1992.

12a. DISTRIBUTION/AVAILABILITY STATEMENT

Unclassified-Unlimited
Subject Category – 08

12b. DISTRIBUTION CODE

13. ABSTRACT ***(Maximum 200 words)***

This paper presents the results of an analytical study conducted to investigate airframe/engine interface dynamics, and the influence of rotor speed variations on the flight dynamics of the helicopter in hover, and to explore the potential benefits of using rotor states as additional feedback signals in the flight control system. The analytical investigation required the development of a parametric high-order helicopter hover model, which included heave/yaw body motion, the rotor speed degree of freedom, rotor blade motion in flapping and lead-lag, inflow dynamics, a drive train model with a flexible rotor shaft, and an engine/rpm governor. First, the model was used to gain insight into the engine/drive train/rotor system dynamics and to obtain an improved simple formula for easy estimation of the dominant first torsional mode, which is important in the dynamic integration of the engine and airframe system. Then, a linearized version of the model was used to investigate the effects of rotor speed variations and rotor state feedback on helicopter flight dynamics. Results show that, by including rotor speed variations, the effective vertical damping decreases significantly from that calculated with a constant speed assumption, thereby providing a better correlation with flight test data. Higher closed-loop bandwidths appear to be more readily achievable with rotor state feedback. The results also indicate that both aircraft and rotor flapping responses to gust disturbance are significantly attenuated when rotor state feedback is used.

14. SUBJECT TERMS	15. NUMBER OF PAGES
Flight dynamics, RPM variations, Rotor state feedback	46
	16. PRICE CODE: A03

17. SECURITY CLASSIFICATION OF REPORT	18. SECURITY CLASSIFICATION OF THIS PAGE	19. SECURITY CLASSIFICATION OF ABSTRACT	20. LIMITATION OF ABSTRACT
Unclassified	Unclassified		